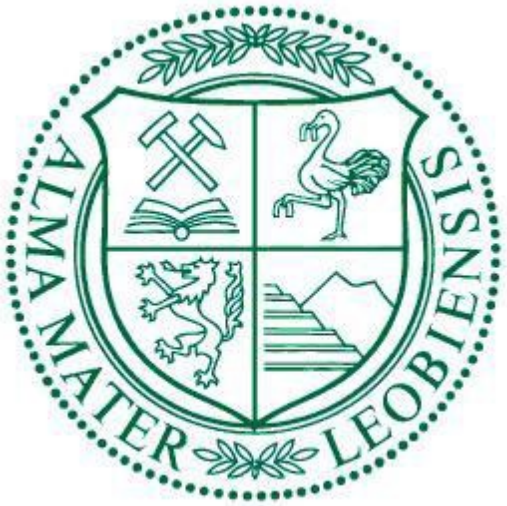

Master Thesis

Verification of a Methodology of Permeability Upscaling using Wavelets

Written by:
Masoumeh Mofarrah, BSc
0735475

Advisor:
Prof. Dr. Stephan K. Matthäi

Abstract

Fluids in petroleum reservoir flow on a wide variety of physical scales. This behavior is one of the challenging problems, which occurs in modeling and simulation of reservoirs. As there is a large difference between geological characterization and smallest grid size in numerical simulation, the detailed fine models cannot be used directly for numerical simulation. The problem of multiple scales can be solved by using some upscaling or homogenization procedure, in which the reservoir properties are represented by averaged properties and the flow is solved on a coarse grid. In recent years, different upscaling procedures have been developed. Wavelet transformations are one of those methods, which are known as the most efficient method that is being adopted for a vast number of applications such as compression and transformation of data.

This master thesis represents the verification of the wavelet transformation in property upscaling of two (2D) and three-dimensional (3D) fine scale geocellular model.

In this work, wavelet transformation is applied to scale up the fine property data from “Tenth SPE Comparative Solution Project: A Comparison of Upscaling Techniques”, which has been published in public domain. The effects of this method on the fine model in terms of the number of blocks, oil in place, pore volume, saving CPU time and memory storage especially on 3D is going to be investigated. In this thesis, behavior of wavelet transformation is studied through upscaling in 2D and 3D. Different coarsening ratios are applied to get coarse models. Then both fine and coarse models are simulated in Petrel with different scenarios to see the flow displacement efficiency of the models.

2D fine scale model has 60 x 220 x 1 cells (13,200 cells), due to size of the model, it is implemented easily in Petrel. The upscaling results are perfectly matched with fine model simulation results. 3D upscaling is applied on two models. Smaller model has 60 x 220 x 20 cells (264,000 cells) and is a sector model of the original SPE 10’s model (85 layers). Properties are scaled up with different coarsening ratios. Observable simulation consequences demonstrate that there is a good match between fine and coarse simulation results. Second model has 60 x 220 x 85 cells (1,122,000 cells) which it is full original SPE 10’s model. Properties are upscaled with a coarsening ratio and simulation results of coarse model are compared with the fine and results presented in the paper. The comparison results show that, there are no significant differences between this study and those, which obtained in the SPE 10 paper.

Kurzfassung

Der Fließvorgang des Lagerstättenfluids findet auf unterschiedlichen physikalischen Ebenen statt. Diese Tatsache ist eine der Herausforderungen die beim Modellieren/Simulieren zu berücksichtigen ist. Das geologische Model, das auf einem feinem Grid-Model aufgebaut ist, repräsentiert die geologische Variation innerhalb einer feinen Skalierung. Dieses Model kann nicht direkt für die nummerische Simulation herangezogen werden. Das Problem das durch die Mehrfachskalierung hervorgerufen wird kann einerseits durch einige Up-scaling Vorgänge oder durch Homogenisierung behoben werden. Beim Up-scaling Vorgang wird Werte der gemittelte Lagerstättenparameter herangezogen und anschließend der Fluidfluss basierend auf einem groben Grid simuliert. Verschiedene Up.scaling Prozeduren wurden in den vergangenen Jahren entwickelt. Die Wavelet-Transformation ist zur Zeit die effizienteste Methode, wenn eine große Datenmende wie z.B. Kompressionsdaten und Transformationsdaten zum Einsatz kommen. Die vorliegende Master Thesis stellt die Verifikation der Wavelet Transformation bei einem angemessenen Up-scaling von einen 2D /3D fein skaliertem Geocelluar-Modell dar. In dieser Arbeit wird für das Up-scaling des feinmaschigen Modells die Daten von der Veröffentlichung “Tenth SPE Comparative Solution Project: A Comparison of Upscaling Techniques”, die Wavelet transformation angewendet. Die Auswirkungen auf dieses “Fine model” in Hinblick auf die Anzahl der Blöcke, Oil in Place, Porenvolumen, CPU-Zeit und die Speicherkapazität insbesondere bei 3D wurden analysiert. In dieser Arbeit wurde das Verhalten der Wavelet Transformation anhand eines Up-scaling in 2D und 3D untersucht. Für die Erstellung des Coarse-Modells wurden unterschiedliche Coarse-Ratios herangezogen. Anschließend wurden das feine und grobmaschige Modelle in Petrel importiert und verschiedenen Scenarien simuliert, mit dem Ziel die Effizienz der Verdrängung des Fluids zu beobachtet. Das 2D Fine Scale Model ist aus 60 x 220 x 1 Zellen (13,200 Zellen) aufgebaut und aufgrund der Größe konnte es leichter in Petrel implementiert werden. Die Up-scaling Ergebnisse sind übereinstimmend mit dem Simulationsergebnisse des Fine-Modells. 3D Up-scaling wurde auch an beide Modelle angewendet. Das kleinere Modell hat 60 x 220 x 20 Zellen (264,000 Zellen) und ist ein Teilmodel des SPE 10’s Model (85 Schichten). Die Eigenschaften wurden einem Up-scaling mit

unterschiedlichen Coarsing Ratio´s unterzogen. Die beobachteten Resultate der Simulation dokumentieren, dass eine gute Übereinstimmung zwischen dem feinen und dem groben Simulationsmodel vorliegt. Das zweite Model besteht aus 60 x 220 x 85 Zellen (1,122,000 Zellen) und ist eines der Originalmodel aus dem SPE 10's Model. Die Eigenschaften wurden dem "Up-scale" Verfahren unterzogen unter Anwendung verschiedenen Coarsing Ratio´s. Anschließend wurden die Simulationsergebnisse zwischen den unterschiedlichen Gridtypen verglichen und die Ergebnisse in der Arbeit präsentiert. Der Vergleich der Resultate belegt, dass es keine signifikanten Änderungen zwischen der vorliegenden Studie und den bereits veröffentlichten Studien gibt.

EIDESSTATTLICHE ERKLÄRUNG

Ich erkläre hiermit an Eides statt, dass ich diese Arbeit selbständig, andere als die angegebenen Quellen und Hilfsmittel nicht benutzt und mich auch sonst keiner unerlaubter Hilfsmittel bedient habe.

AFFIDAVIT

I declare in lieu of oath, that I wrote this thesis and performed the associated research myself, using only literature cited in this volume.

Datum/date	Unterschrift/ signature

DEDICATION

This thesis is dedicated to my parents for their love, endless support, and encouragement and also to my brothers, specially Dr. Ramin Mofarrah and his family for their great support.

ACKNOWLEDGEMENT

I would like to express my gratitude to Professor Stephan K. Matthaei for his supervision and guidance for this thesis.

My utmost gratitude to Dr. Siroos Azizmohammadi, for his supervision, that truly helped me during the project.

I am also grateful to Dipl. Ing. Georg Zangl from FRD Company and Dipl.-Ing. Philip Mähr. A good contribution from both of them during the four months is great indeed.

At least but not the least I want to thank my friends specially Dr. mont. Dipl. Ing. Ataollah Javidi and colleagues at FRD Company, who appreciated and motivated me, that made all the things possible.

Nomenclatures

Symbol	Definition
x	Real variable
$f(x)$	A given function
a	Scale parameter
b	Translation parameter
ψ	Wavelet functions or mother wavelet
K_{rw}	Water relative permeability
K_{ro}	Oil relative permeability
S	Saturation
S_{wc}	Connate water saturation
S_{or}	Residual oil saturation
S_{wi}	Irreducible water saturation

Table of contents

List of figures

List of Table

1 Introduction

Simulation of multiphase flow processes, such as oil and gas recovery is one of the challenging subjects. A large difference between geological characterization and smallest grid size in numerical simulation is one of the main sources of this challenge (Nordbotten et al., 2010).The detailed fine models cannot be used directly for numerical simulation because of high CPU time, computational effort and huge storage capacity (Babaei and King, 2011; Shehata et al., 2012).

Flow simulation is usually performed on a scale that is much coarser than the scale of the direct or indirect measurements. In the other hand grids, which are used to reservoir description are too fine to be used in reservoir simulators (Christie, 1996). Risk and uncertainty assessment are another issues in reservoir performance in deterministic models and can be measured by simulation of different scenarios. Thousands of such runs may be required to cover the range of parameter variations. These simulations are not feasible on fine grid model and are more complicated and time consuming (Panda et al. 2000; Durlofsky, 2005; Sahimi et al., 2005; Babaei and King, 2011). This problem can be solved by smaller-size representations of reservoir models that best mimic the large size model in simulation output (Babaei and King, 2011).

Upscaling is the methodology for transferring the properties from a fine scale to a coarse scale with an appropriate number of cells for reservoir simulation. (Panda et al. 2000; Shehata et al., 2012), and provides suitable values for porosity, permeability and other flow characteristics (Christie, 1996).

1.1 Literature Review

In recent years, different upscaling procedures have been developed. The main reason to generate a coarse model refers to keep the fine scale geological description in flow simulation. Some researchers (Barker and Thibeau, 1997; Barker and Dupouy, 1999; Farmer, 2002; Darman et al., 2002; Gerritsen and Durlofsky, 2005; Chen, 2005) developed and described the variety of upscaling methods and their applications.

Upscaling techniques can be classified in terms of the types of parameters that are upscaled (single or two phase flow parameter upscaling) and according to the

problems, solved to determine the coarse-scale parameters. In particular, methods may be categorized as local, extended local, quasi-global or global (in order of increasing computational effort) depending on the problem solved in the upscaling computations (Panda et al. 2000; Gerritsen and Durlofsky, 2005; Chen and Durlofsky, 2007). More discussion that is detailed and classification for upscaling techniques can be found in Durlofsky (2005). For moderate degree of coarsening, single phase upscaling techniques and for higher degree due to different geological facies, beside absolute permeability, two additional properties are needed to be upscaled: relative permeability and capillary pressure (Panda et al. 2000; Durlofsky, 2005). In general, two-phase upscaling methods are more computationally expensive than single-phase upscaling procedures (Chen and Durlofsky, 2007). Level of accuracy and degree of upsaling are important factors, which represent efficiency of an appropriate upscaling approach. For example for permeability with two-point geostatistics and with a moderate degree of coarsening, the use of local single-phase upscaling procedures may provide acceptable coarse models. For some cases which are more challenging with e.g., channelized systems extended local or (quasi) global single phase upscaling coupled with two-phase upscaling may be necessary (Chen and Durlofsky, 2007).

In a purely local procedure, only the fine scale region corresponding to the target coarse block is coarsened (Durlofsky, 1991; Pickup et al., 1994b; King and Mansfield, 1999; Durlofsky et al., 2000; Gerritsen et al., 2006; Lambers et al., 2008) while in extended local procedures, regions neighboring the coarse block are included as well. In other words, the regions corresponding to the target coarse block plus a fine scale “border region" or skin around this region is considered. This calculation is performed by averaging the fine scale solution (e.g., pressure and velocity) only over the region corresponding to the target coarse block (Holden and Lia, 1992; Wen et al., 2003; Durlofsky, 2005; Chen, and Durlofsky, 2007). In both approaches, boundary conditions, which are imposed on the fine scale regions, are Neumann or periodic boundary conditions (Durlofsky, 1991; Pickup et al., 1994b; Wen et al., 2003b). A big issue in any local or extended local upscaling technique is the choice of boundary conditions. Because the actual conditions imposed on the region during the flow simulation are not known and will vary (Durlofsky, 2005). Although local

methods results are satisfactory for some reservoirs, they generally do not perform well when the spatial scales of reservoir heterogeneities, such as high-permeability flow paths are larger than the simulation grid (Gerritsen and Lambers, 2008). Global methods, which use global fine-scale flow simulations to determine coarse-scale parameters, can reduce errors of large connected flow paths, but they are generally expensive (White and Horne 1987; Holden and Nielsen, 2000; Durlofsky, 2005; Mallison et al., 2006; Zhang et al., 2008). In quasi-global upscaling techniques, that refers to as “local-global” methods (Chen et al. 2003; Chen and Durlofsky 2006a), a global coarse-scale simulation is used in order to determine the boundary conditions for the local fine-scale calculation of permeability or transmissibility. The global coarse simulation and local fine-scale calculations are repeated until a consistency of solution is achieved. This method shows much more accuracy for difficult problems with highly heterogeneous channelized systems and changing flow conditions (Wen et al., 2006).

It is said, that there are two different local-global procedure in 2D systems: one of them refers to generic global boundary conditions (Chen et al. 2003) and the other is called “adaptive local-global” (ALG) procedure, that uses specific global boundary conditions and/or wells and adapted for any type of global flow (Chen and Durlofsky 2006a). An alternative approach to upscaling, which improves the precision of fluid recovery estimates compared to conventional coarse grid simulation is dual mesh technique. This method using considerably less CPU time and memory than a full fine scale simulation (Ramè and Killough, 1991; Guérillot and Verdière, 1995; Guedes and Schiozer, 1999; Gautier et al., 1999; Audigane and Blunt, 2003, 2004).

Several different methods also have been proposed over time. The simplest analytical methods are arithmetic, geometric, and harmonic averaging, which are based on the concepts of parallel and serried connections of the upscaled parameters (Warren and Price, 1961; Wen and Gómez-Hernández, 1996; Renard and Marsily, 1997). Other methods, which try to account for the basic physics of the flow in several dimensions, are like the renormalization and the tensor methods transformation (King et al., 1993; Christie et al., 1995; King, 1988, 1989, 1995, 1996; Jansen and Kelkar, 1998).

Numerical methods provide better performance to handle complex heterogeneities, but may be computationally demanding. On the other hand, analytical methods are usually restricted by simplifying assumptions but less expensive and faster than numerical methods in terms of computational cost. Numerical methods however are more general and can be used on any permeability field (Lee et al., 1996).

In addition, there is some limited research on wavelet upscaling method. Wavelet transforms (WT) includes multi-resolution analysis (MRA) properties that leads to have inherent multi-level bases, compact support, and (semi-) orthogonality principle. These features provide an attractive framework for data representation and numerical solution of differential equations (Moridis et al. 1996; Panda et al. 2000) also analyzing of data distribution at different resolutions at the same time (Mallat, 1989). This idea is not new. It has existed since the early 1800's, when Joseph Fourier could superpose sines and cosines to represent other functions (Graps, 1995). Wavelet analysis is also a powerful tool to integrate different types of information, e.g., prior geological information, 3-D seismic data, and well logging data (Lu and Horne, 2000).

Due to the above properties and advantages over trigonometric series, wavelets have been used in different cases and have fast become a popular tool for the analysis of non-stationary signals, image processing, time frequency decomposition and many more applications. Several authors like Daubechies (1992), Mallat (1989, 2009) and Vetterli et al. (1992) have described the construction of wavelets and their applications.

1.2 Claim

Through this study, I aim to understand the Verification of a Methodology of Permeability Upscaling using Wavelets. The performance of the wavelet upscaling method will be investigated for the highly heterogeneous fine model, which has been provided by the SPE10 paper (Christie and Blunt, 2001). To evaluate the method, the number of blocks, oil in place, saving CPU time and memory storage especially on 3D is going to be investigated and simulation results of fine and coarse model are compared.

The wavelet upscaling code, used in this study has been developed by Dr. Siroos Azizmohammadi in C++. It does a flexible multilevel upscaling for highly

heterogeneous porous rocks in full 3D and layer-by-layer, 2D cut plane in any desired direction (x, y, z) and also Local Grid Refinement (LGR) for predefined regions.

1.3 Agenda

In chapter 1, an Introduction to upscaling and a literature review are presented. Chapter 2 presents the methodology, which includes the explanation of wavelet upscaling and geological fine and coarse models with different scenarios. Chapter 3 is the presentation of upscaling and simulation results, which are later discussed in chapter 4. Conclusions are addressed in chapter 5.

2 Methodology

The upscaling method that is applied in this study is based on wavelet transformation, which had success in developing in relation to wide range of applications in physics, signal/image processing and mathematics over the last two decades. This conventional method is a general tool to analyze multi-resolution problems that provides an alternative to decompose a signal or data set in scale-space and allows for the gradual smoothing of a set of data by removing high frequency features (Jansen and Kelkar; 1998; Panda et al. 2000; Azizmohammadi and Matthäi, 2011). WTs have been used in the petroleum industry (Guan et al., 2004) and mostly for the analysis of temporal data and 2D or higher-dimensional reservoir description (Guan et al., 2004; Jansen and Kelkar, 1998; Panda et al., 2000). WT can be thought as a linear filter in 1-D and an array of different sized filters in 2- and 3-D, which can be used to scan the data for small and large events. This method is able to keep principle structural features and is well suited for upscaling rock properties in a multiscale heterogeneous porous media (Chu, et al. 1996; Jansen and Kelkar; 1998; Panda et al. 2000; Azizmohammadi and Matthäi, 2011; Babaei and King, 2011).

Wavelet Transform is a linear transformation and its coefficients are linear combinations of parameters in the real space. Compared to the traditional trigonometric with sine and cosine basis functions the wavelet bases are localized at both frequency and space scale, this allows for compact support of functions, such as the wavelet functions defined by Daubechies (1992) in Figure 2.1. With any changes such as shock wave in a function, only local coefficients in wavelet approximation will be affected and no global cancellation is needed (Moridis et al., 1996).

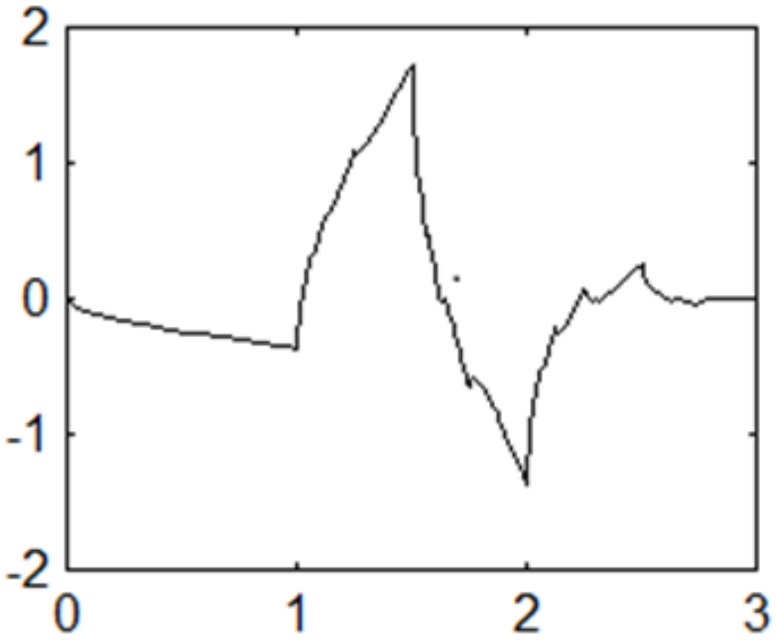

Figure 2.1. Daubechies - 4 wavelet (Tanyel, 2006).

The transform do not act like the Fourier operation. This is refers to this fact, that Fourier transform gives the information of certain frequencies and this information cannot be effectively used, as it is not spatially localized (Azizmohammadi et al., 2007).

The basic mechanism of the WT can be defined by the integral representation of functions. Moreover, the measurement of permeability and porosity as hydrological properties is represented by averaging behavior around a point of interest (Panda et al., 1996). It can be defined by a physical instrument, which is an integral measure and is given by a convolution of a given function $f(x)$ with a kernel function ψ_{ab} as follows:

$$F(a,b) = \int_{-\infty}^{+\infty} f(x)\,\psi_{ab}(x)dx \quad (1)$$

Where x is a real variable, α is a scale parameter, b is a translation parameter, and the family of functions $\psi_{ab}(x)$ are called wavelet functions or mother wavelet as:

$$\psi_{ab(x)} = \frac{1}{\sqrt{|\,a|}}\psi\left[\frac{x-b}{a}\right] \quad (2)$$

Where $a>0, -\infty < b < \infty$, small values of $|\,a|$ correspond to high frequencies. By setting, $|\,a\,|$, the dilation can be changed. For high frequency ψ_{ab} will be narrow, and

for low frequency ψ_{ab} is wide. In Figure 2.1 wavelet was shown at both a high (to the right) and a low (to the left) frequency. It can be seen also that the high frequency wavelet is more compact than the low frequency, which causes the wavelet to be fitted exactly to the proper scale of the data corresponding to the frequency (Jansen et al., 1998; Azizmohammadi et al., 2007).

The advantage of representation of functions refers to its possibility to extract different local characteristics of $f\ (x)$ by choosing an appropriate value of kernel ψ_{ab} in Eq. 1. For example, with a kernel function ψ_{ab}, that is nonzero only over a finite interval and sums to 1, so Eq. 1 gives the local average of $f\ (x)$ around the location x .On the other hand, if ψ_{ab} sums to zero then the integral in Eq. 1 evaluate the deviation of $f\ (x)$ from its local mean (Panda et al., 2000). In this method alternatively, the permeabilities of the coarsened blocks can be specified by calculating of average permeability of the original fine-scale blocks.

Wavelet upscaling method performs the coarsening process in such a way that the distribution of block permeabilities in the coarsened model automatically follows closely to the original fine-scale model (Azizmohammadi et al., 2007).

2.1 Model set up

All models of 2D and 3D are created based on SPE 10's model. The essential data to set up the models is obtained from "Tenth SPE Comparative Solution Project: A Comparison of Upscaling Techniques" (Christie and Blunt, 2001).

2.1.1 2D Upscaling model

The fine geological model scale in our study is described on a regular Cartesian grid. It is created from 3D fine model, which is described in the next section for each individual layer and has 60 x 220 x 1 cells (13,200 cells). It is made in software Petrel. The coarse model has same created structure with the fine model but it contains different properties. In other hand, the coarse model is the fine model with the properties upscaled based on wavelet upscaling algorithm. In order to investigate the performance of this method, first, the maps of fine and coarse models are compared visually, afterwards, they are simulated and the simulation results e.g.

pressure, oil production rate, cumulative oil production and water cut of field for both models, are reported for 2000 days of production.

In accordance with wavelet transformation, each property can be scaled up with different threshold numbers, which leads to different compression percentage. Threshold here is related to the cut off concept in reservoir engineering. Generally, formation cutoffs are applied as limiting values, which are used to eliminate formation intervals and they do not contribute significantly to the storage and productive reservoir capacity.

Fine porosity and permeability in each case is upscaled in two consequence levels. In the next step in order to simulate the models, the following scenario is defined: some required data to set up this mode is different form 3D models. Initial pressure and depth are defined 121 bar and 1220 m respectively. Those fine and coarse models involve two injectors and three producers. The wells are vertical and completed by perforating the casing. Injectors are located on the left side and near top and bottom of the model and the producers are located on the right side of the model. The location of wells is shown in Table 2.1.

Table 2.1. Well location data (Christie and Blunt, 2001).

Well name	**X** Location [m]	**Y** Location [m]
Injection Well $INJ1$	105	457
Injection Well $INJ2$	46	168
Production Well $PROD1$	262	412
Production Well $PROD2$	268	36
Production Well $PROD3$	293	256

Five strategies are defined for the simulation scenario:

1. Groups (field) rate production control. The oil rate for this group is assumed 403.4 sm^3/d. According to this strategy, filed is controlled by its production rates of oil, water, gas, liquid and reservoir volume rates to meet the predefined oil production rate.

2. Well rate production control for producers; this strategy implies that, production wells are controlled by maximum limits on oil production rate. The oil production rate in this strategy is assumed 80.7 sm^3/d.
3. Well pressure production control for producers; based on this definition, producers are controlled by minimum limits on flowing bottom hole or tubing head pressure. Bottom hole pressure for this strategy is defined 34.5 bar.
4. Well water injection control for injectors; water injection wells are controlled by bottom hole pressure. This parameter is assumed 310.3 bar.
5. Group voidage replacement injection rule. This rule controls injection to replace production voidage. Voidage replacement refers to replacing the volume of oil, gas, and water produced from the reservoir by injecting fluids.

The map of the model including five wells is illustrated in Figure 2.2.

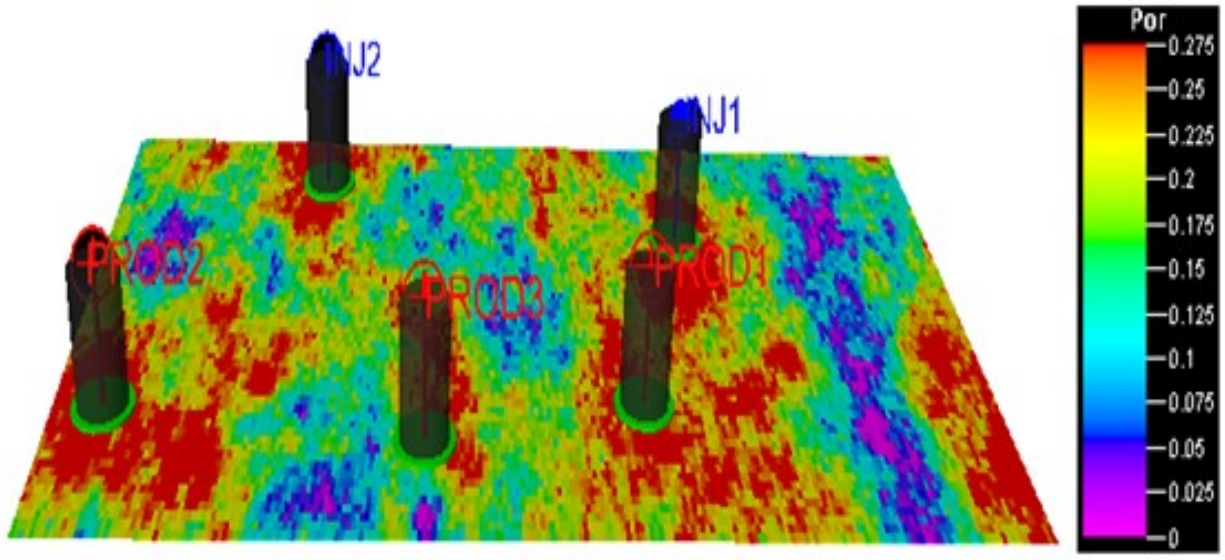

Figure 2.2. Porosity map for 1 - Layer sub model of SEP's 10 model.

2.1.2 3D Upscaling model

3D upscaling is applied on two models. Smaller model has 20 layers, 60 x 220 x 20 cells (264,000cells) with 6.09 m x 3.03 m x 2.6 m (20 ftx 10 ftx 8.5 ft) cell size and it is a cut off model of the original SPE 10 (85 layers). This fine model is created in Petrel and afterwards to build a coarse model, first porosity and then permeability are upscaled with different threshold numbers by WT and imported to Petrel as well. Flow

displacement behavior is being studied through different scenarios. To investigate the results of simulations for both models, different coarsening ratios are chosen.

To set up this model, some data such as number of layers, cell size, and the injection rate have been reported different from the paper. The cell size in z-direction is defined 2.6 m instead of 0.61 m, since 0.61 m is compatible with the given depth, PVT and well configuration data, which were defined for 85 layers. Well types and the well location data are other information needed to set up the model as well. All models include one injector and four producers, which are vertical and completed throughout formation. The needed information to set up the model has been described below.

- **Relative permeabilies:**

$$K_{rw} = \left(\frac{S - S_{wc}}{1 - S_{wc} - S_{or}}\right)^2$$

$$K_{ro} = \left(\frac{1 - S - S_{or}}{1 - S_{wc} - S_{or}}\right)^2$$

$$S_{wc} = S_{wi} = S_{or} = 0.2$$

$$K_{rw}(S_{or}) = K_{ro}(S_{wc}) = 1.0$$

Where K_{rw} is water relative permeability and K_{ro} is oil relative permeability. S,S_{wc} ,S_{or} and S_{wi} are saturation, connate water saturation, residual oil saturation and irreducible water saturation respectively.

Table 2.2. Relative permeabilities (Christie and Blunt, 2001).

Sw	Krw	Kro
0.200	0.0000	1.0000
0.250	0.0069	0.8403
0.300	0.0278	0.6944
0.350	0.0625	0.5625
0.400	0.1111	0.4444
0.450	0.1736	0.3403
0.500	0.2500	0.2500
0.550	0.3403	0.1736
0.600	0.4444	0.1111
0.650	0.5625	0.0625
0.700	0.6944	0.0278
0.750	0.8403	0.0069
0.800	1.0000	0.0000

Table 2.3. Water properties (Christie and Blunt, 2001).

	$C_w[Pa^{-1}]$	Viscosity $[Pa.s]$
1.01	0.021	0.0003

Table 2.4. Dead oil and PVT data (Christie and Blunt, 2001).

P $[bar]$	B_o	Viscosity $[Pa.s]$
20.69	1.05	0.00285
55.16	1.02	0.00299
551.59	1.01	0.00300

- **Initial condition**
  - initial pressure: 413.69 $[bar]$
  - Initial depth: 3657.6 $[m]$
  - Surface densities: oil: 849 $[kg/m^3]$; water: 1025.18 $[kg/m^3]$
  - Rock compressibility: 00.6897 $[Pa^{-1}]$

- **Well configuration**
  - All wells are vertical and completed throughout formation
  - For central Injector, Injection rate is 794.94 [$\frac{sm^3}{day}$] (reservoir conditions) and Maximum injection bottom hole pressure assumed 689.5 [bar]
  - 4 producers Produce at 276 [bar] bottom hole pressure

Table 2.5. Well location data (Christie and Blunt, 2001).

Well name	$\boldsymbol{X}$ Location [m]	$\boldsymbol{Y}$ Location [m]
Injection Well $I1$	183	335
Production Well $P1$	0	0
Production Well $P2$	366	0
Production Well $P3$	366	671
Production Well $P4$	0	671

To investigate the performance of the method, pressure, oil production rate, cumulative oil production, and water cut of the field for both fine and coarse models after 2000 days of production is simulated. In addition, a comparison of oil in place is made between fine and coarse models.

To simulate and to run of the model, simulation strategy is needed to be defined. Therefore, the following development strategies, according to the given data in the paper are applied to the model.

1. Well water injection control, in this strategy, reservoir rate is defined as a control mode and reservoir rate and bottom hole pressure are assumed 477 sm^3/d and 276 bar .
2. Well pressure production control for producers, bottom hole pressure is considered here as a control mode and its value is assumed 276 bar.

This section of 3D upscaling consists of four trials of different simulation scenarios and also different coarsening ratios in order to investigate.

Injection rate for 85 layers was reported 794.94 sm^3/d in the paper. Due to inappropriate result especially for pressure, different values e.g., 636 sm^3/d, 477sm^3/d , 318 sm^3/d and 238 sm^3/d are checked out to set an appropriate value and finally 477sm^3/d is chosen for the first trial. After simulation the fine model and run of this model, in the next step and for upscaling, porosity and permeability are

scaled up with different ratios. (In this report, permeabilites in 2 directions x and y were considered same values). Afterwards the coarse model is simulated with above scenario and with the properties, scaled up by 0.52 and 0.8 threshold numbers. It should be noted, due to some issue while the program was running, the number of days to run the coarse models were less than 2000 days.

For the second trial, some parameters in development strategy are changed and two strategies are defined. Well rate production control for producers is the first strategy. In this definition oil rate as a control mode is assumed 129 sm^3/d for producers 1, 2, and 3 and 44.5 sm^3/d for producer 4. In the second strategy, the group voidage replacement injection rule is added. As it mentioned in 2D upscaling, this rule controls injection to replace production voidage. Also due to variation of properties as they are upscaling, Petrel calculates automatically new productivity index after each simulation. The new values are different from its value of the fine model. To avoid this difference a default value as a fix value for both cases is defined. In addition, well locations are considered as fine grids while the areas between the wells are presumed as coarsened grid cells. This step involved upscaling of the fine model with threshold numbers 0.5, 0.51, 0.6, and 0.68. Among the above numbers, threshold numbers 0.5 and 0.68 give better results than other ratios. To improve the results and for the third trial, the new feature of the program in which, properties are scaled up layer by layer is used. To run the model, the essential data is not changed and the results are checked up with different threshold numbers. Among different numbers, Numbers 0.6 and 0.8 are chosen to represent the simulation outcomes. The new obtained results except in pressure case look better than previous ones.

In the final step, the WCONPROD keyword is replaced with a new definition in Eclipse data files. This keyword defines control data for production wells. Like previous procedure and with the same data and threshold numbers the outputs of simulation can meet expected results. The map of the model including the wells is shown in Figure 2.3.

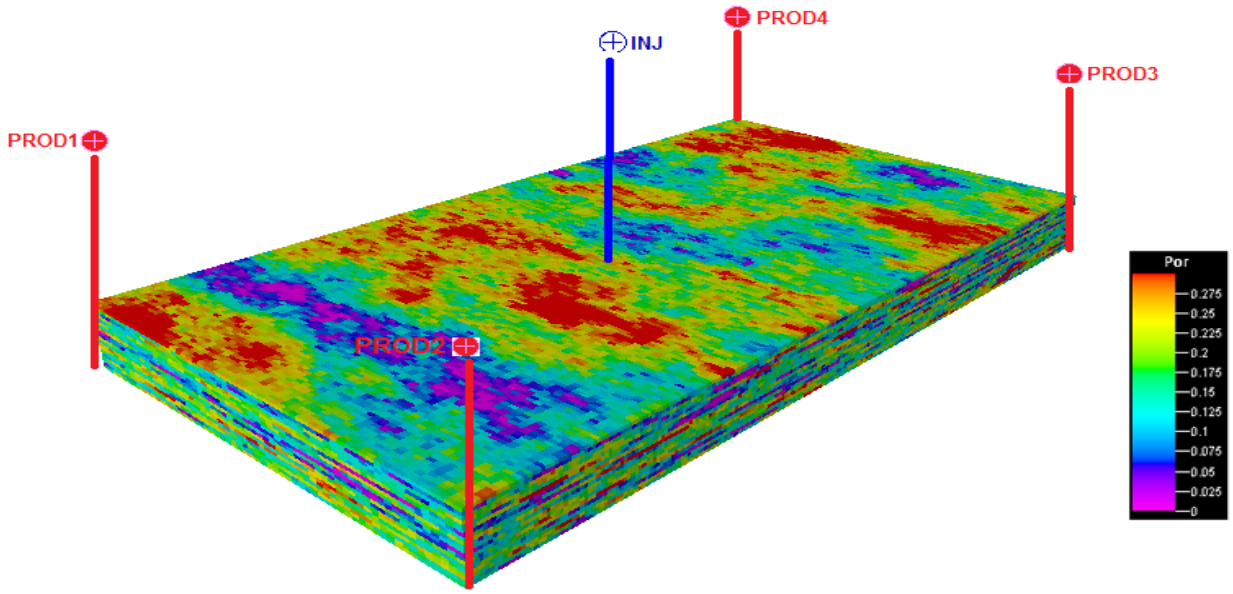

Figure 2.3. Porosity map for 20 – Layers – sub model of SPE's 10 model.

Second model has 60 x 220 x 85 cells (1,122,000 cells) which it is full original SPE 10's model. The description of this model and required data to set up are similar to the model of 20 layers. Like the previous procedure, this fine model is built in Petrel and then in order to build a coarse model, at first porosity and then permeability are upscaled by WT with threshold Number of 0.8 and then they are imported to the E&P software; Petrel. Due to the large volume of the cells with 85 layers and facing problem while running, FrontSim Schlumberger simulator is chosen to run this simulated model. Since it can perform simulations on large and complex reservoir models several orders of magnitude faster than standard finite difference simulators.

The main purpose of this part of thesis, despite its running difficulties, is comparing of simulations results with some simulators outcomes, mentioned in SPE 10 paper. Two simulators Chevron and TotalFinaElf, which assumed single-phase upgridding like WT method in their upscaling procedure, are chosen for my study.

Chevron used different coarsening strategies to ensure reasonable agreement on quantities of interest. This resulted in a coarse grid size of 22 x 76 x 42. TotalFinaElf adopted a strategy with assumption of incompressible and single-phase flow. After several different testing, 10 x 37 x 13 was resulted in a coarse grid size (Christie and Blunt, 2001). For more investigation, field average pressure, oil production rate, cumulative oil production, and water cut of the producer 1 like the paper for fine and

coarse models are simulated and run after 2000 days of production. In addition, a comparison of oil in place (OIP) is made between the fine model and WT coarse model.

This model is set up like the 20 layers model but there is difference in their simulation strategy definition. In this step to make a strategy for simulation of the fine model, according to the given data in the paper, the following development strategies are defined:

1. Well water injection control, in this strategy, reservoir rate is defined as a control mode and reservoir rate and bottom hole pressure are assumed 477 sm^3/d and 276 bar .
2. Well pressure production control for producers, bottom hole pressure is considered here as a control mode and its value is assumed 276 bar.

After simulation and run the fine model, for upscaling, porosity and permeability are scaled up with threshold number 0.8. Afterwards the coarse model is simulated with above scenario and run in FrontSim. The map of the fine model is illustrated in Figure 2.4.

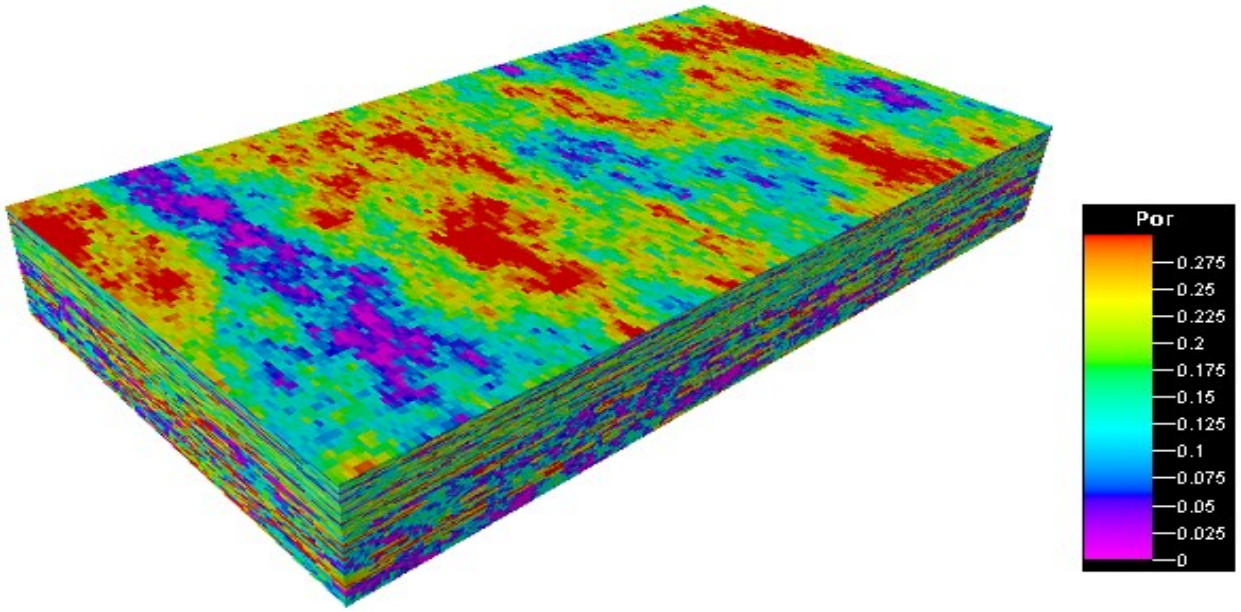

Figure 2.4. Porosity map for 85 - Layers original model of SEP's 10 model.

3 Results

As mentioned in the methodology section, upscaling in 2D and 3D led to the following results. Flow displacement behavior, which is studied through different scenarios, and the simulations results of both fine and coarse models are shown in the following figures.

3.1 2D Upscaling

The 2D model represents a model with 60 x 220 x 1 cells (13,200 cells). According to the WT method, each property can be scaled up with different coarsening ratios in two levels, and compressed at different percentage.

In the first level, the compression ratio for porosity is 71.89% and the number of grid cells is 3711. These values for both permeabilites; permeability in x and z directions (Perm$x$ and Perm$z$) are obtained approximately 75%, 3318 and 3315 respectively.

In the second level of the upscaling, the compression ratio for porosity is 88.3% and the number of grid cells is 1545. These values for perm$x$ and perm$z$ are obtained 93.5%, 864, and 858 respectively. Figure 3.1 illustrates the comparison of porosity maps for the fine model and the first level of the coarse model and Figure 3.2 shows the comparison of their histogram. In Figure 3.3 to Figure 3.6, the fine and the coarse maps of Perm$x$, their histograms, and corresponding maps of Perm$z$ are represented respectively.

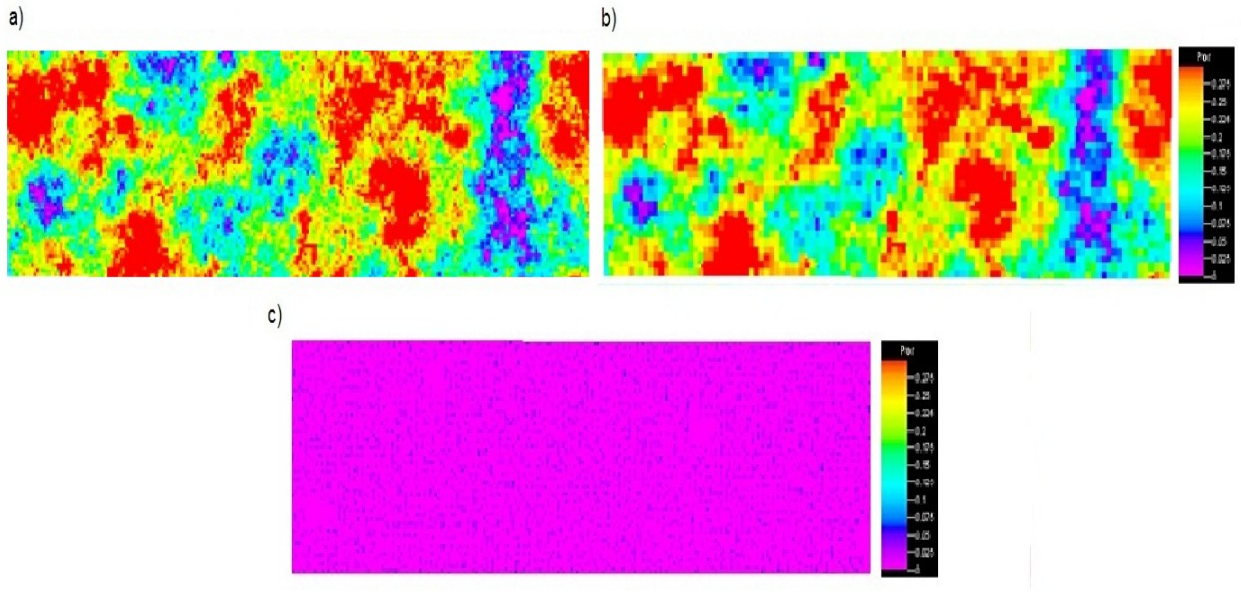

Figure 3.1. Comparison of porosity maps in 1 – Layer Model for (a) Original model. (b) First level upscaling to 13200 grid cells = 3711 grid cells and 71.89% coarsening ratio. (c) Difference between two maps (a) and (b).

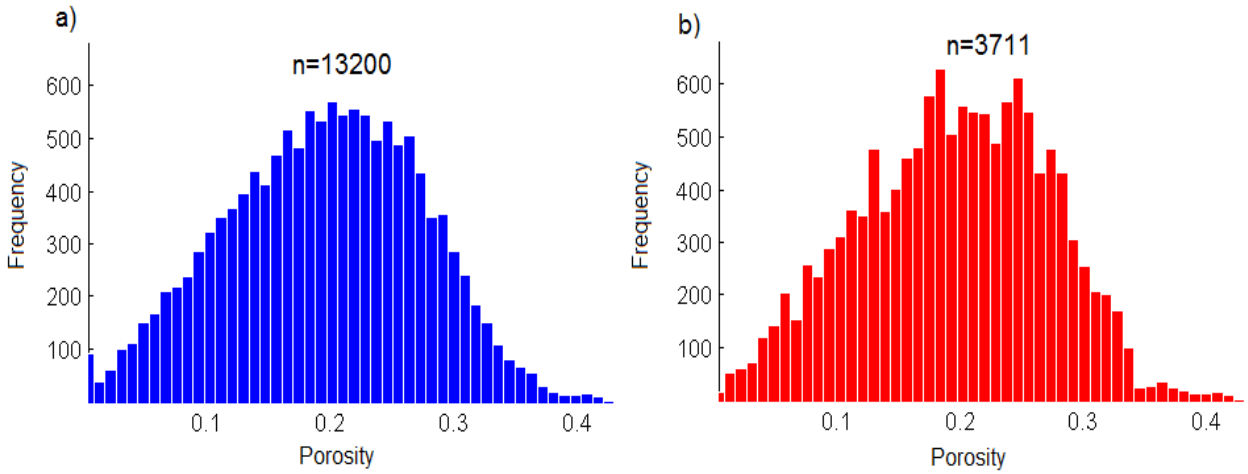

Figure 3.2. Comparison of porosity histograms in 1 - Layer Model for (a) Original model. (b) First level upscaled model.

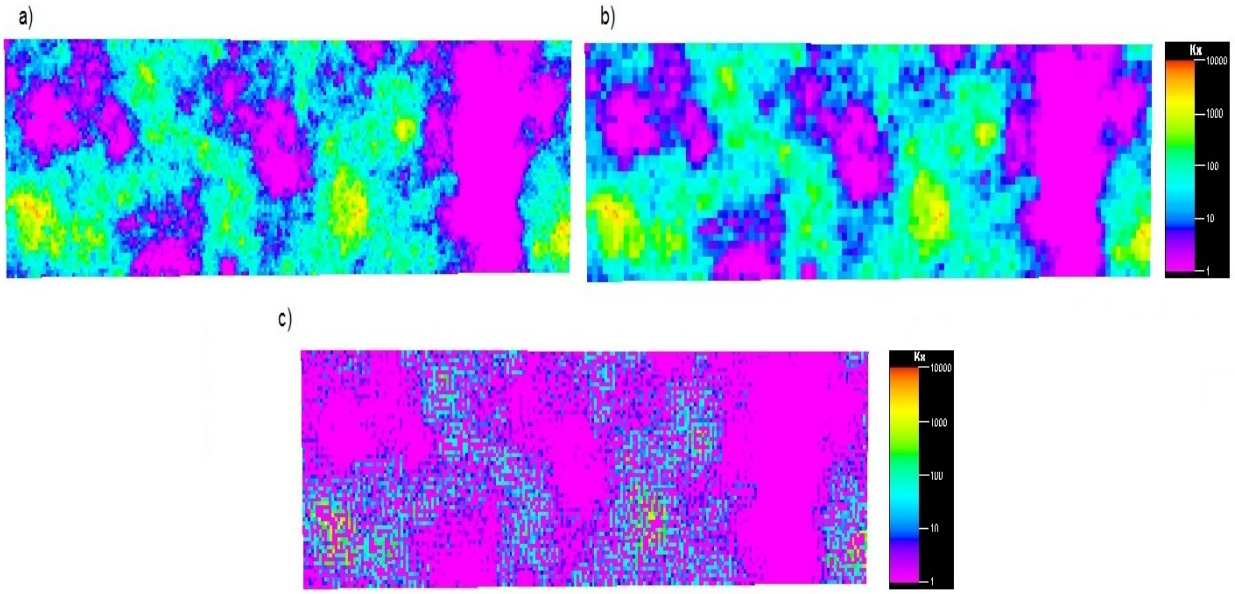

Figure 3.3. Comparison of permeability map in x direction in 1 - Layer Model for (a) Original model. (b) First level model upscaled to 13200 grid cells = 3318 grid cells and 75% coarsening ratio. (c) Difference between two maps (a) and (b).

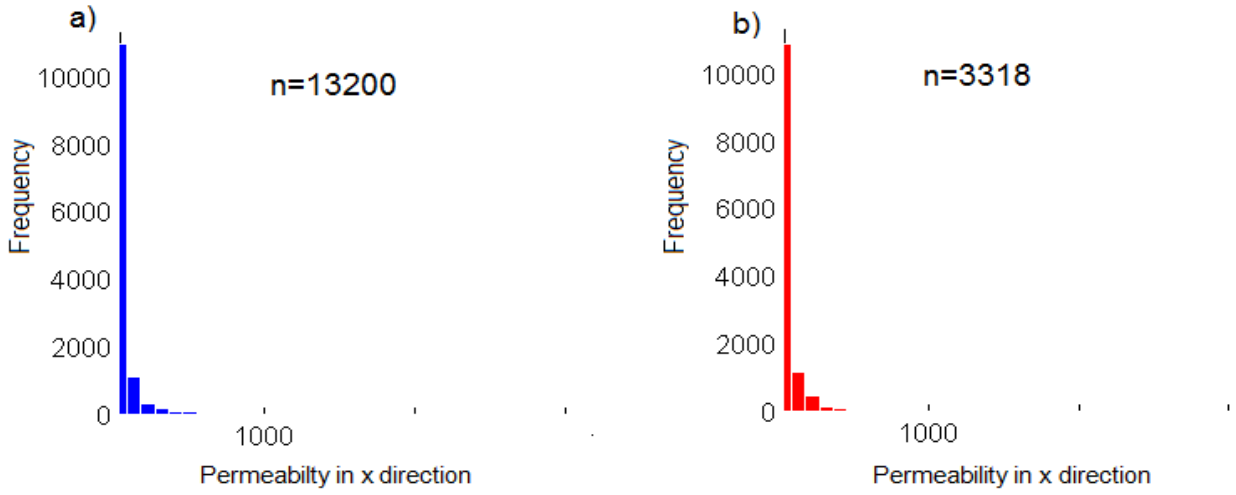

Figure 3.4. Comparison of permeability histograms in x direction in 1 - Layer Model for (a) Original model. (b) First level upscaled model

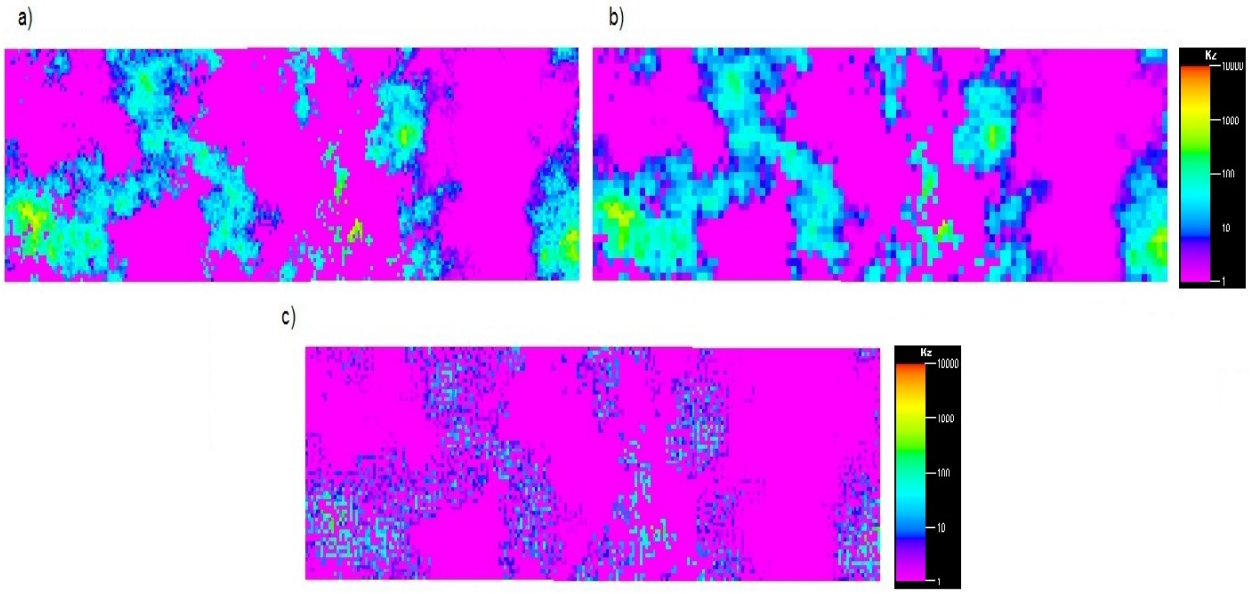

Figure 3.5. Comparison of permeability maps in z direction in 1- Layer Model for (a) Original model. b) Second level model upscaled to 13200 grid cells = 3315 grid cells and coarsening ratio 74.86%. (c) Difference between two maps (a) and (b).

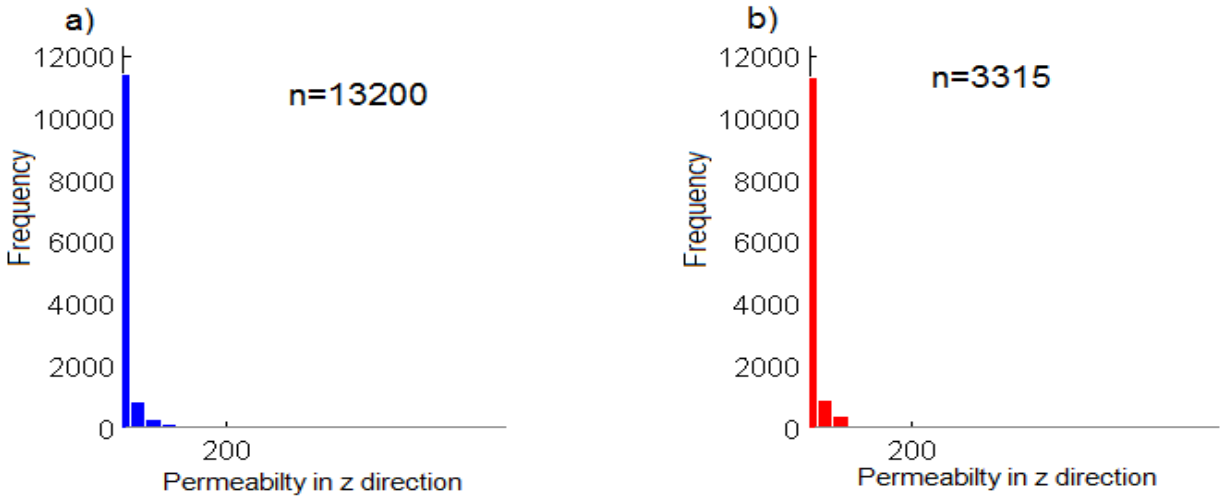

Figure 3.6. Comparison of permeability histograms in z direction in 1 - Layer Model for (a) Original model. (b) First level upscaled model.

Figure 3.7 and Figure 3.8 represent the comparison of porosity maps and their histogram for fine and coarse model of second level and Figure 3.9 to Figure 3.12 show the corresponding maps of Perm$x$ and Perm$z$ respectively.

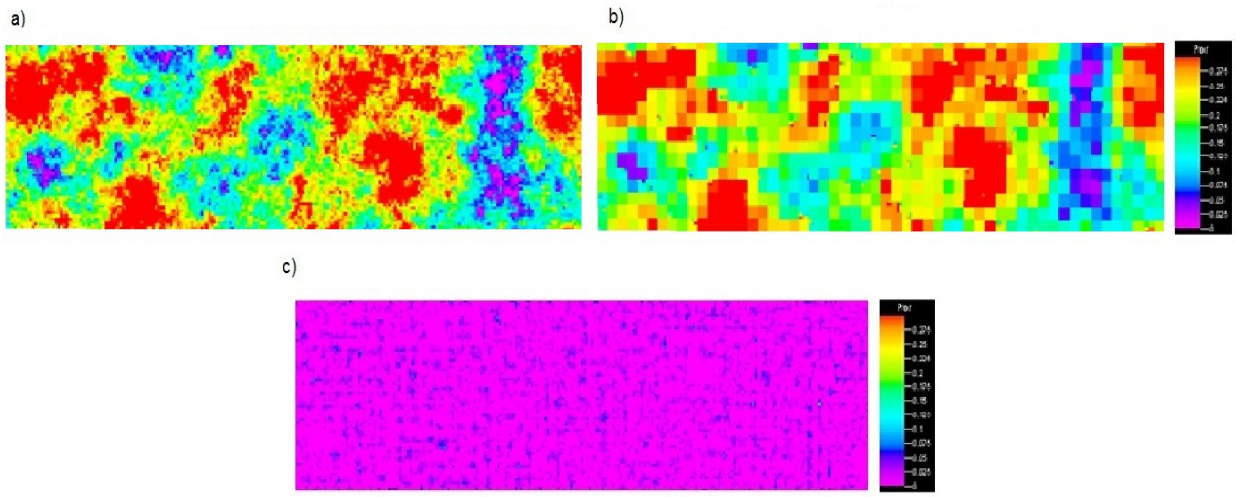

Figure 3.7. Comparison of porosity maps in 1- Layer Model for (a) Original model. (b) Second level upscled model to 13200 grid cells = 1545 grid cells and coarsening ratio 88.3%. (c) Difference between two maps (a) and (b).

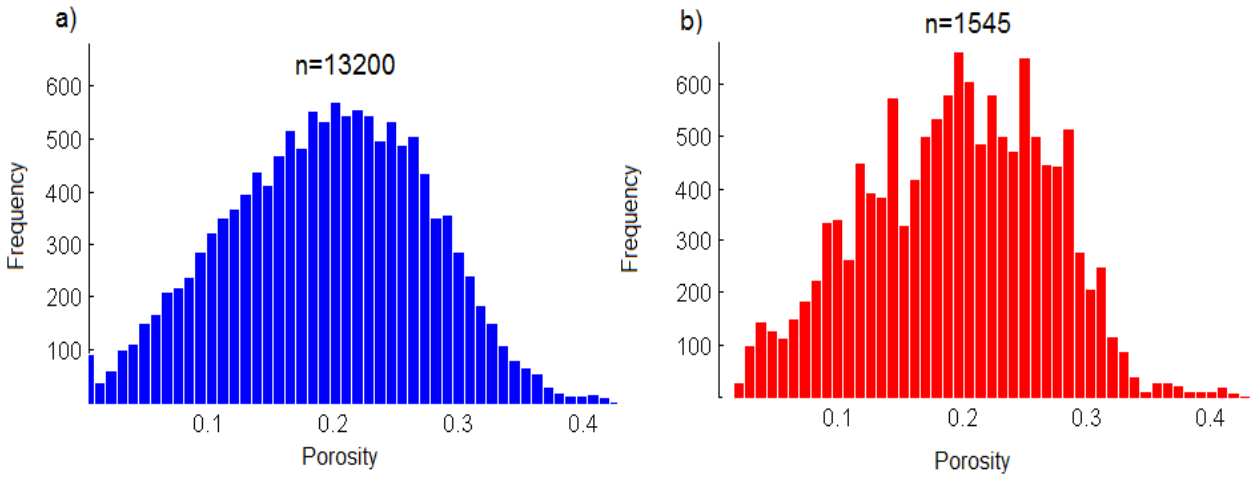

Figure 3.8. Comparison of porosity histograms in 1 - Layer Model for (a) Original model. (b) Second level upscaled model.

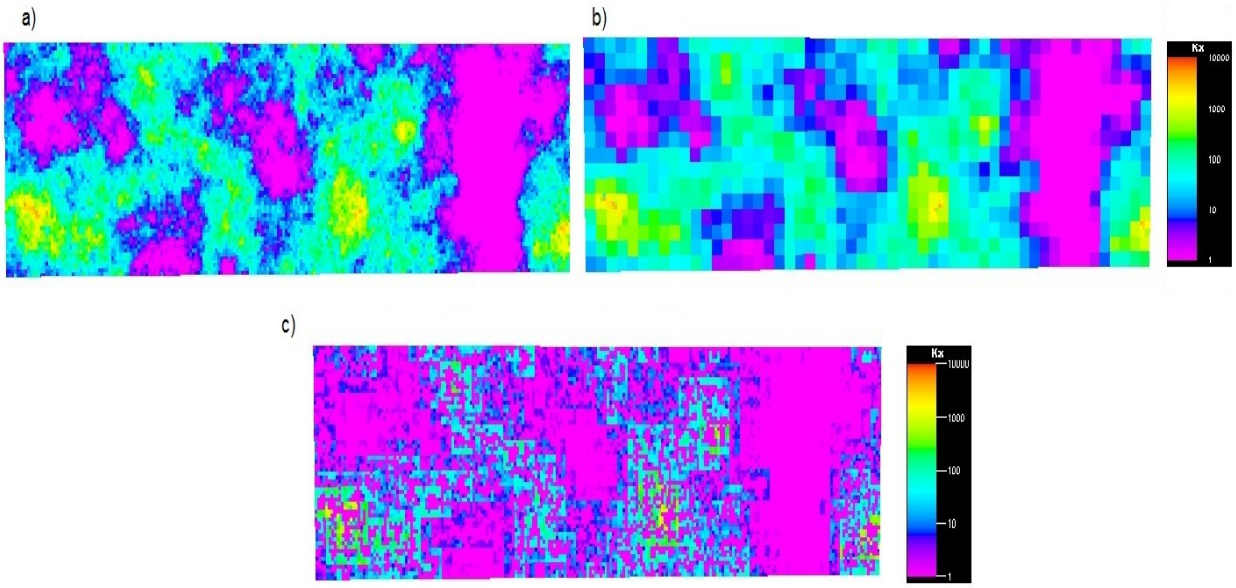

Figure 3.9. Comparison of permeability map in x direction in 1 - Layer Model for (a) Original model. (b) Second level upscaled to 13200 grid cells = 864 grid cells and 93.45%. (c) Difference between two maps (a) and (b).

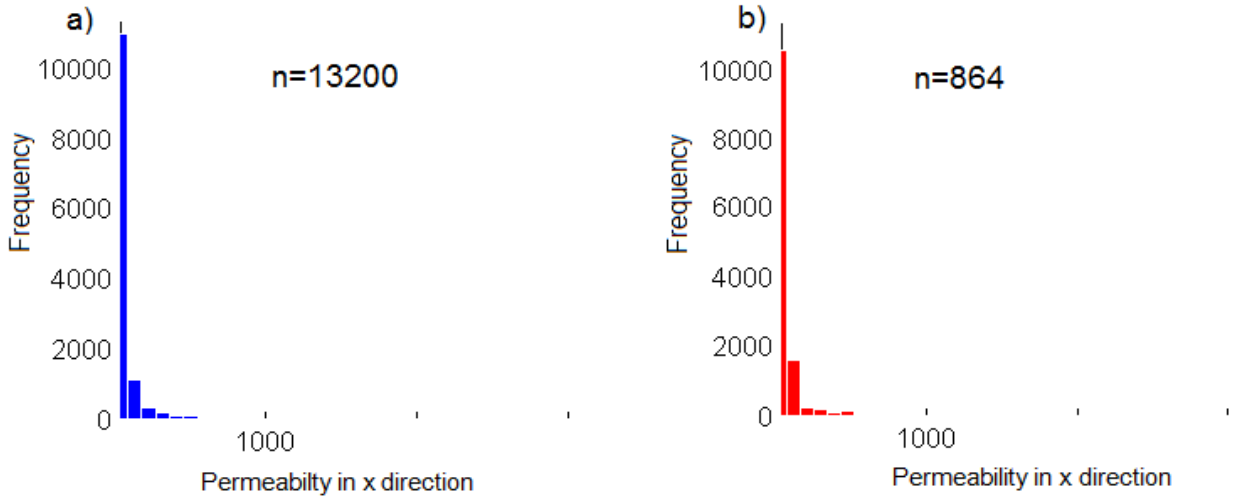

Figure 3.10. Comparison of permeability histograms in x direction in 1 - Layer Model for (a) Original model. (b) Second level upscaled model.

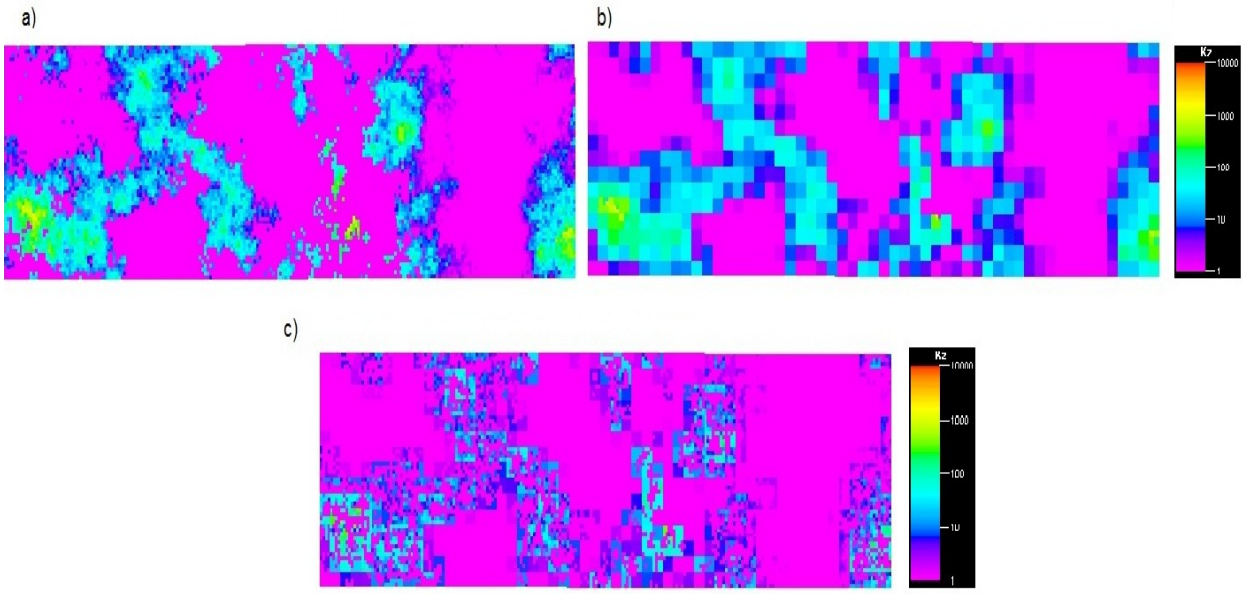

Figure 3.11. Comparison of permeability map in z direction in 1 - Layer Model for (a) Original model. (b) Second level upscaled to 13200 grid cells = 858 grid cells and coarsening ratio 93.5%. (c) Difference between two maps (a) and (b).

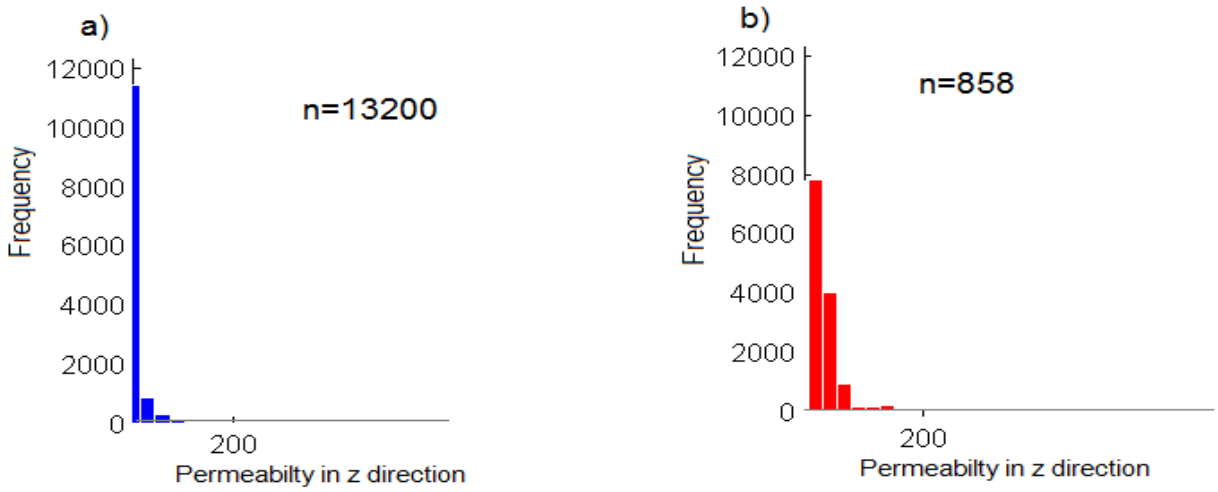

Figure 3.12. Comparison of permeability histograms in z direction in 1 - Layer Model for (a) Original model. (b) Second level upscaled model.

To investigate the performance of the method, field pressure, field oil production rate, field cumulative oil production rate and field water cut for both fine and coarse models for 2000 days of production are simulated. Figure 3.13 to Figure 3.16 represent the results of the simulation. In addition, pore volume changes between both coarse models and fine model and comparison of oil in place for mentioned models are illustrated through Table 3.1 and Figure 3.17.

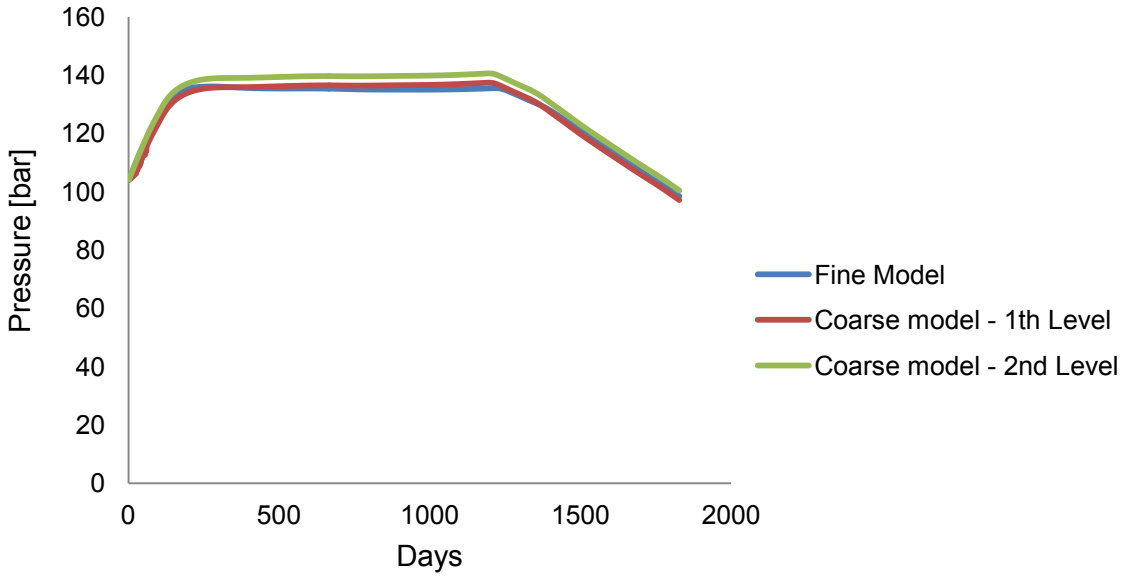

Figure 3.13. Comparison of field average pressure for fine and coarse models of first level and second level.

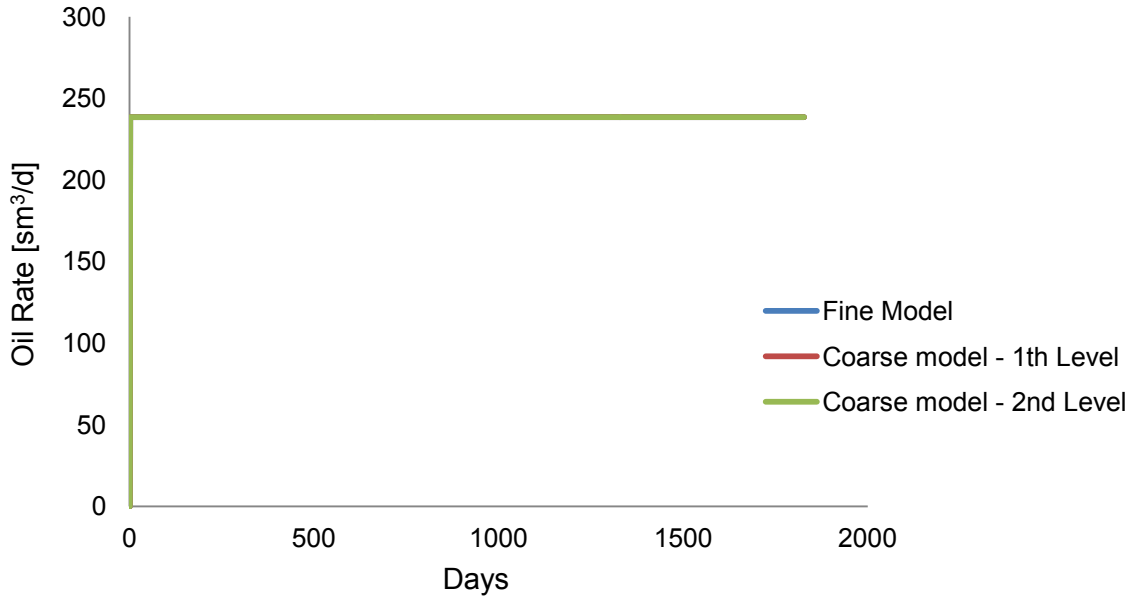

Figure 3.14. Comparison of field oil production for fine and coarse models of first level and second level.

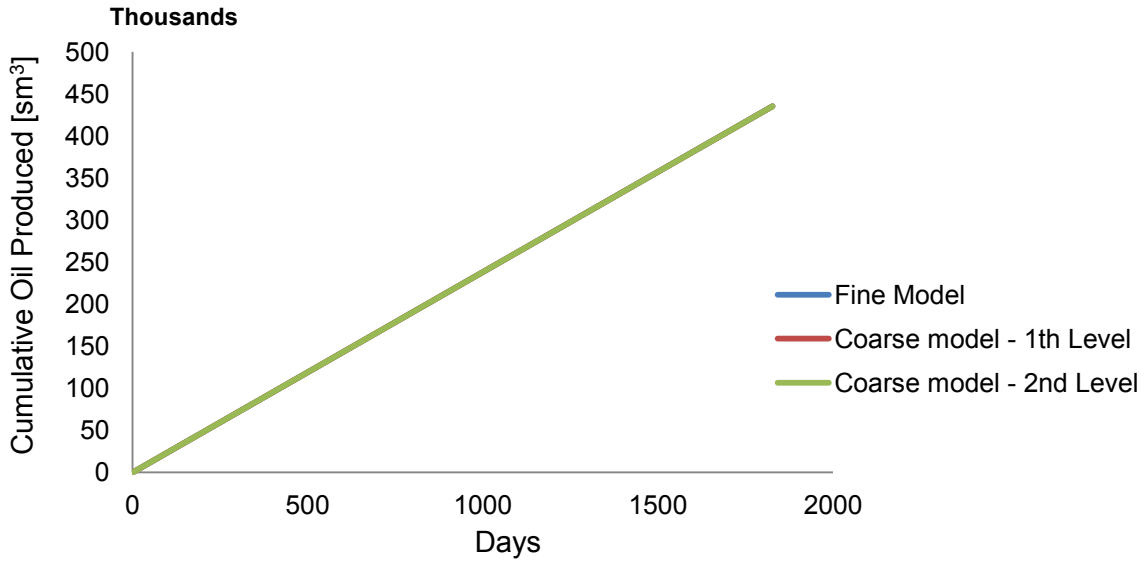

Figure 3.15. Comparison of field cumulative oil production for fine and coarse models of first level and second level.

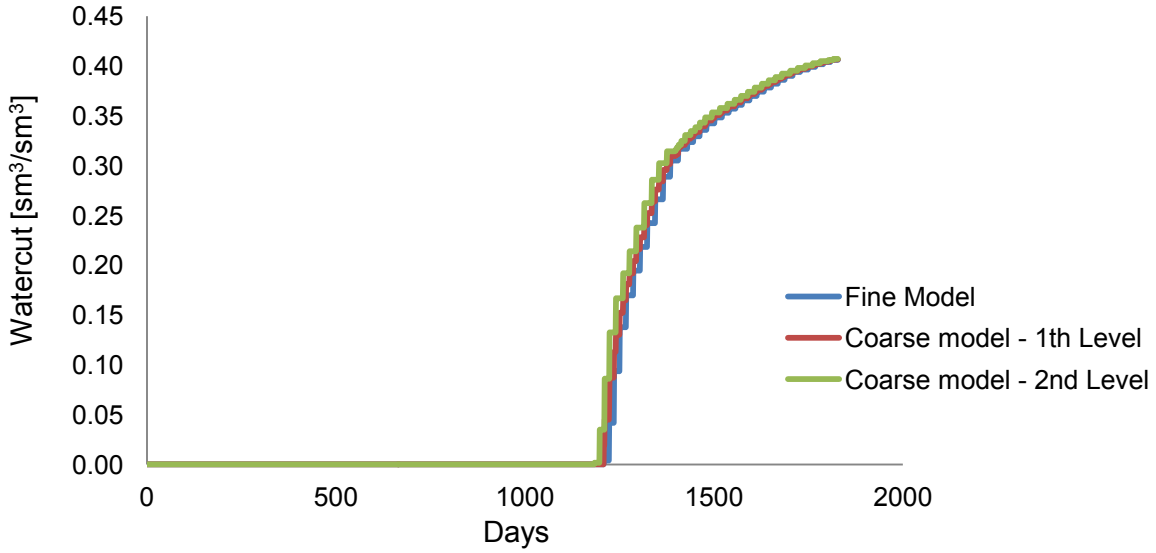

Figure 3.16. Comparison of field watercut for fine and coarse models of first level and second level.

Table 3.1. Comparison of pore volume for fine and 2D coarse models.

Pore volume for 2D model 1-Layer [rm^3]	Difference between fine and coarse model of first level upscaling (%)	Difference between fine and coarse model of second level upscaling (%)
	-0.00177	-0.00187

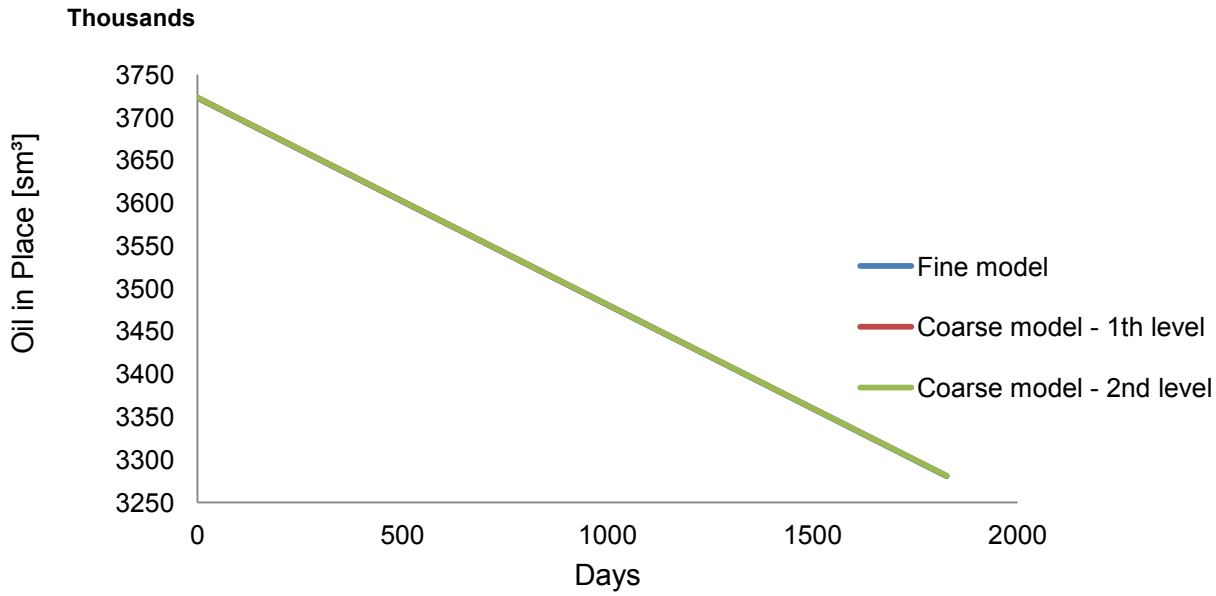

Figure 3.17. Comparison of OIP for fine and coarse models.

3.2 3D Upscaling

Smaller 3D model has 20 layers. Based on the description of the previous section the fine geological model scale in our study is described on a regular Cartesian grid. It has 60 x 220 x 20 cells (264,000cells) and it is a cut off model of the original SPE 10 (85 layers).

In this step, properties are scaled up with different threshold numbers. For the first trial, two coarse models, (1) and (2), are considered, wherein the properties are upscaled with threshold numbers of 0.52 and 0.8. In the coarse model (1), the compression ratio and the number of grid cells for porosity were 5.34% and 249909. These values for both permeabilites; Perm$x$ and Perm$z$ are obtained approximately 76.05%, 63233 and 77.3%, 59915 respectively. In the coarse model (2), the compression ratio and the number of grid cells for porosity were 85.98% and 37011. These values for Perm$x$ and Perm$z$ are obtained approximately 87.2%, 33784 and 87.2%, 33791 respectively. Properties maps of fine and coarse models (1) and (2) also their histograms are compared through Figure 3.18 to Figure 3.29 respectively.

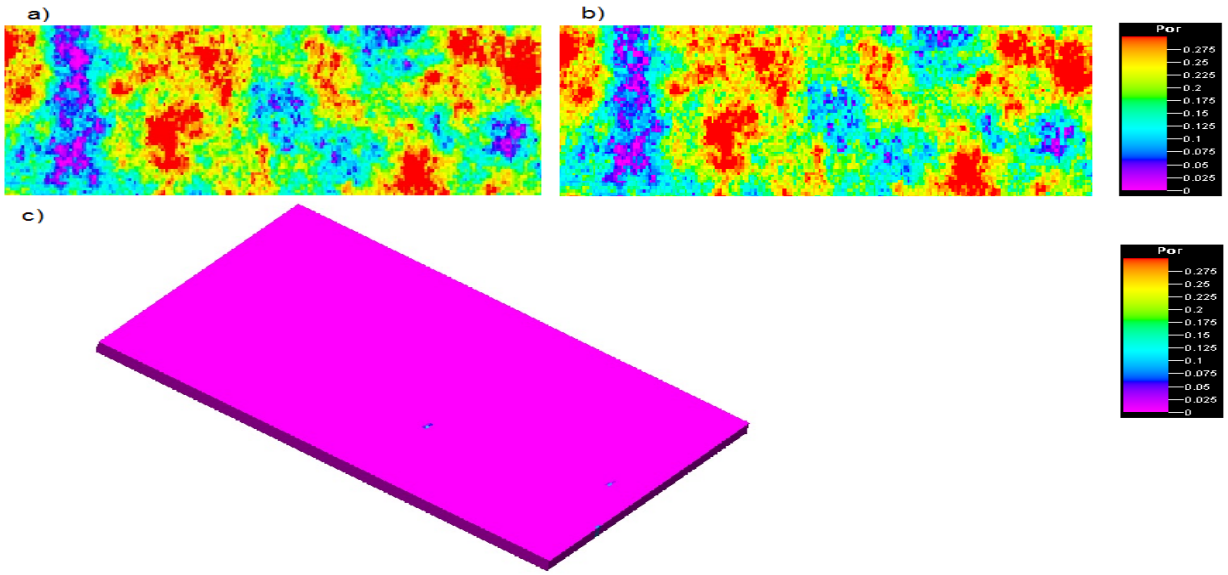

Figure 3.18. Comparison of porosity maps in 20 - Layers Model for (a) Original model. (b) Coarse model (1) upscaled to 264000 grid cells = 249909 grid cells and coarsening ratio 5.34%. (c) Difference between two maps (a) and (b).

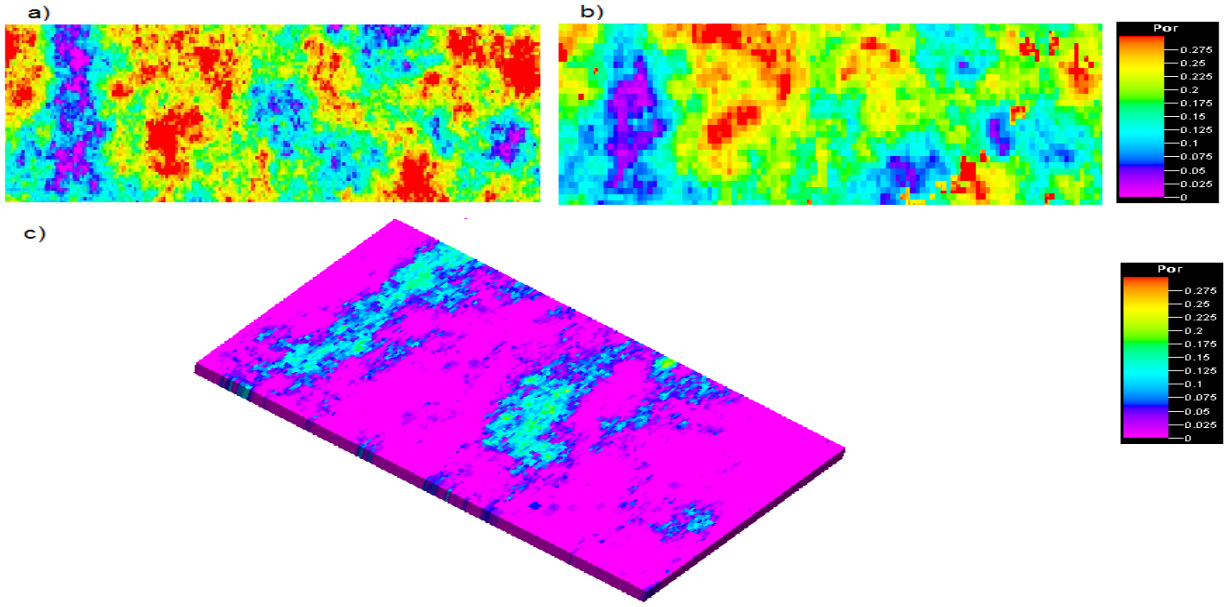

Figure 3.19. Comparison of porosity maps in 20 - Layers Model for (a) Original model. (b) Coarse model (2) upscaled to 264000 grid cells = 37011grid cells and coarsening ratio 85.98%. (c) Difference between two maps (a) and (b).

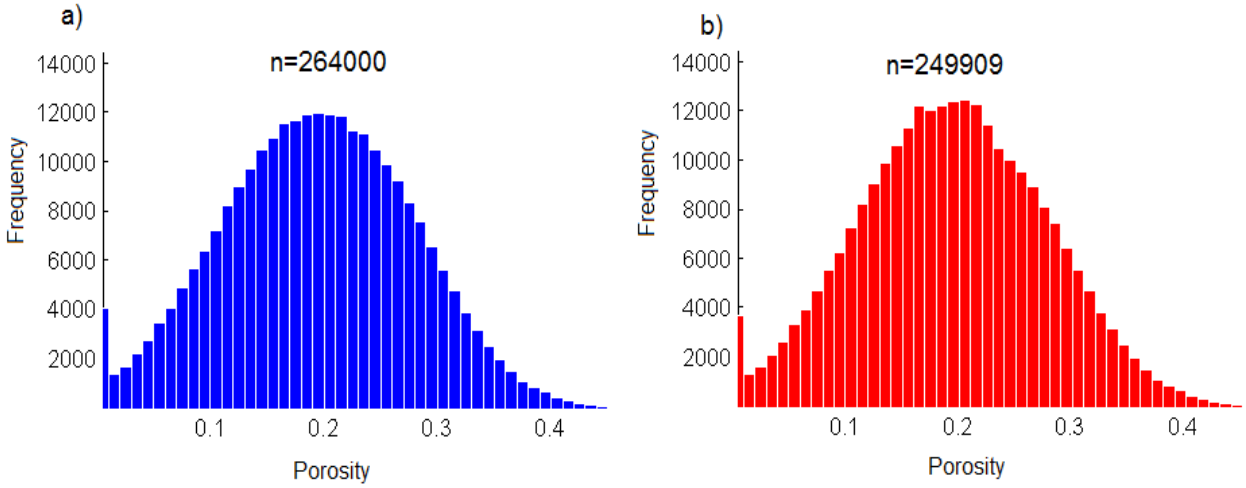

Figure 3.20. Comparison of porosity histograms in 20 - Layers Model for (a) Original model. (b) Coarse model (1).

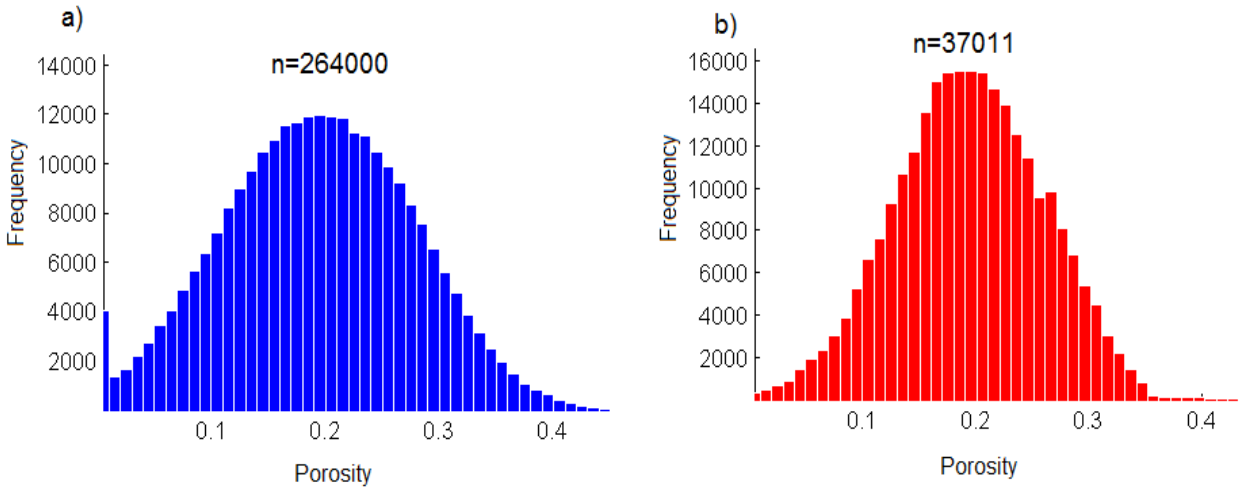

Figure 3.21. Comparison of porosity histograms in 20 - Layers Model for (a) Original model. (b) Coarse model (2).

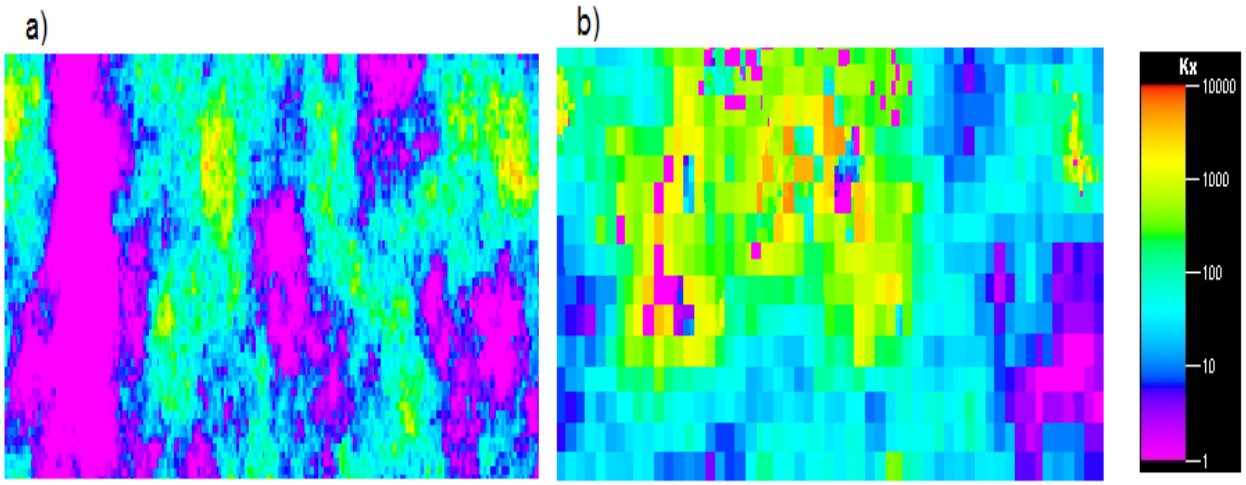

Figure 3.22. Comparison of permeability map in x direction in 20 - Layers Model for (a) Original model. (b) Coarse model (1) upscaled to 264000 grid cells = 63233 grid cells and coarsening ratio 76.05%. (c) Difference between two maps (a) and (b).

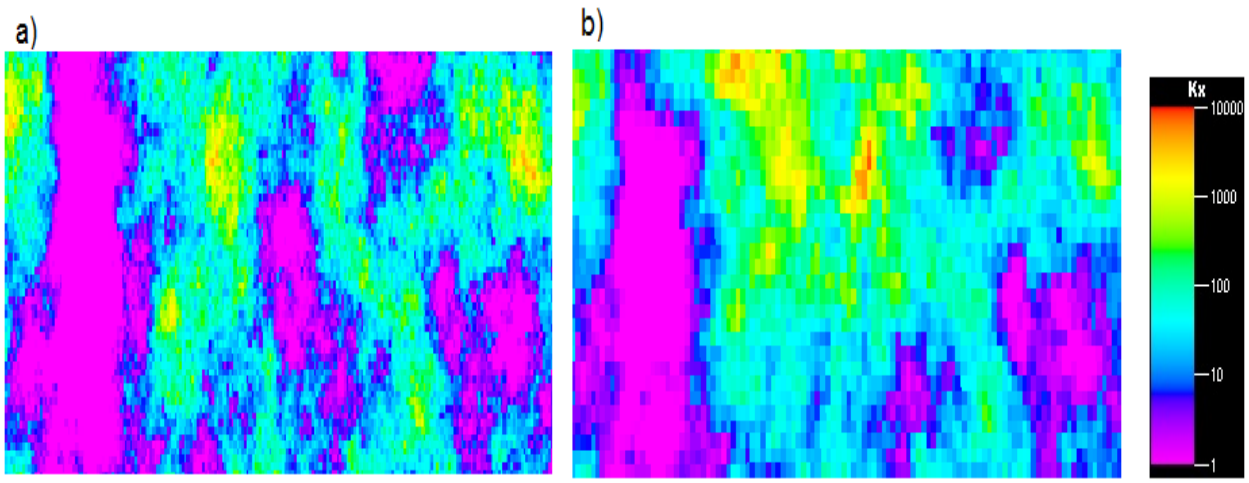

Figure 3.23. Comparison of permeability map in x direction in 20 - Layers Model for (a) Original model. (b) Coarse model (2) upscaled to 264000 grid cells = 33784 grid cells and coarsening ratio 87.2%. (c) Difference between two maps (a) and (b).

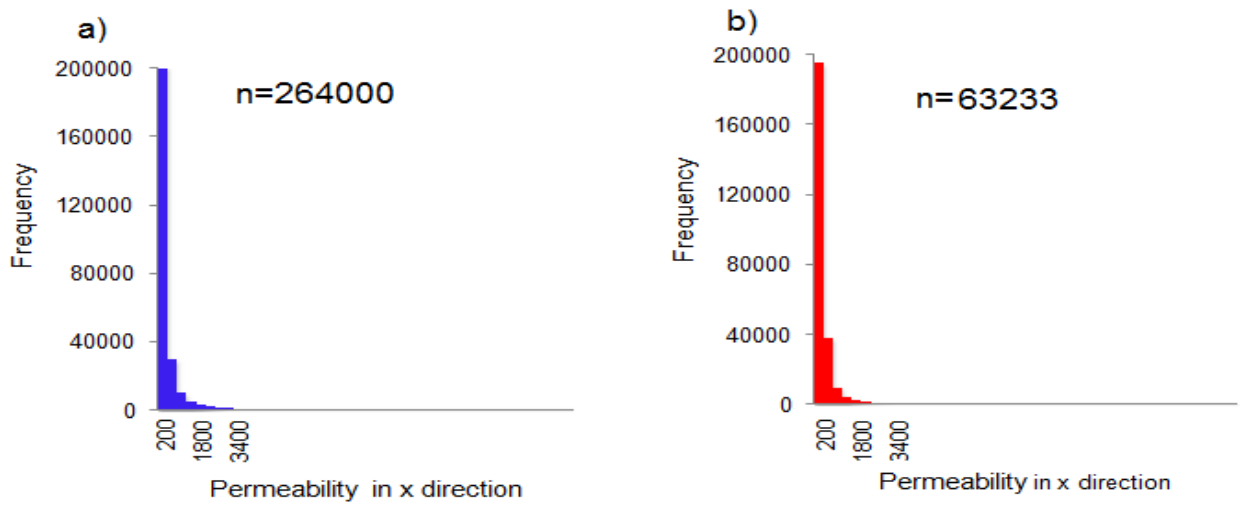

Figure 3.24. Comparison of permeability histograms in x direction in 20 - Layers Model for (a) Original model. (b) Coarse model (1).

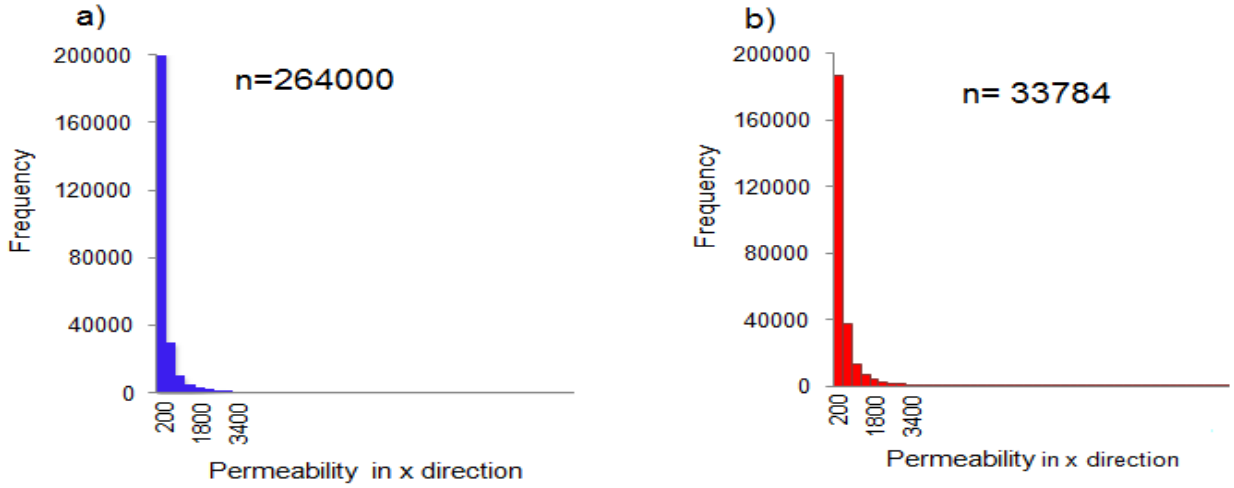

Figure 3.25. Comparison of permeability histograms in x direction in 20 - Layers Model for (a) Original model. (b) Coarse mode (2).

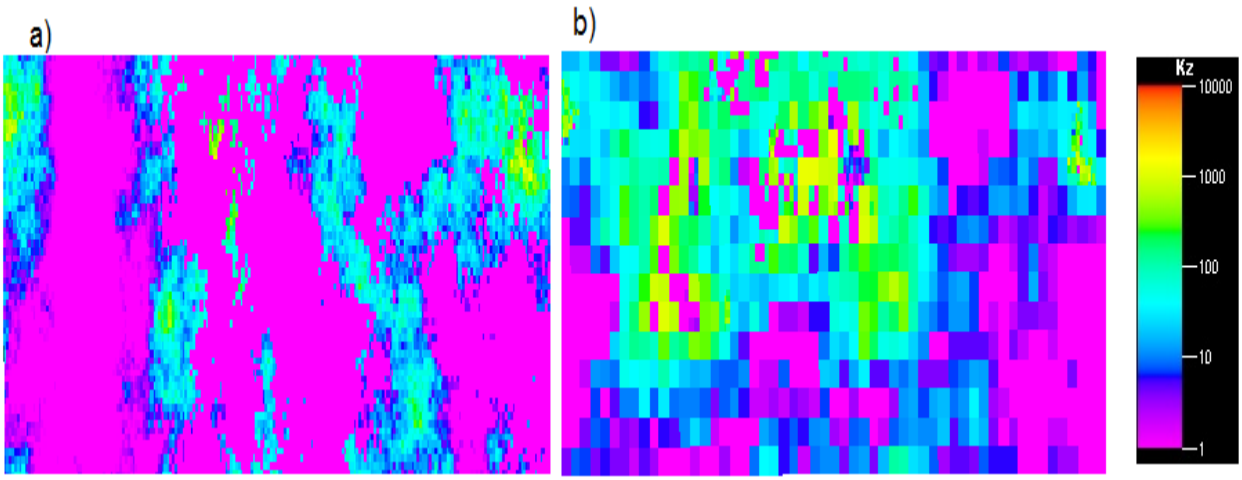

Figure 3.26. Comparison of permeability map in z direction in 20 - Layers Model for (a) Original model. (b) Coarse model (1) upscaled to 264000 grid cells = 59915 grid cells and coarsening ratio 77.3%. (c) Difference between two maps (a) and (b).

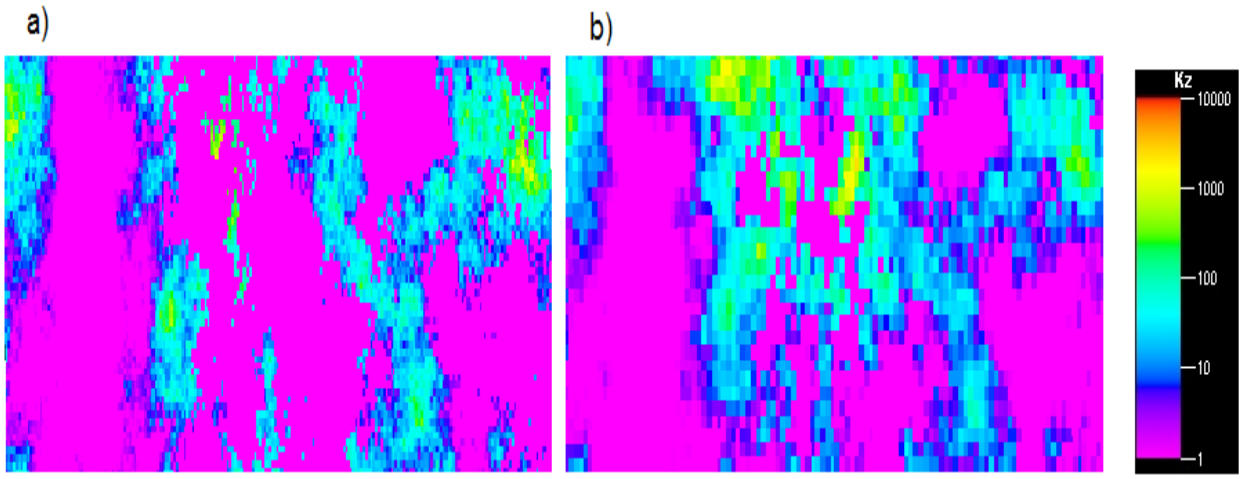

Figure 3.27. Comparison of permeability map in z direction in 20 - Layers Model for (a) Original model. (b) Coarse model (2) upscaled to 264000 grid cells = 33791 grid cells and coarsening ratio 87.2%. (c) Difference between two maps (a) and (b).

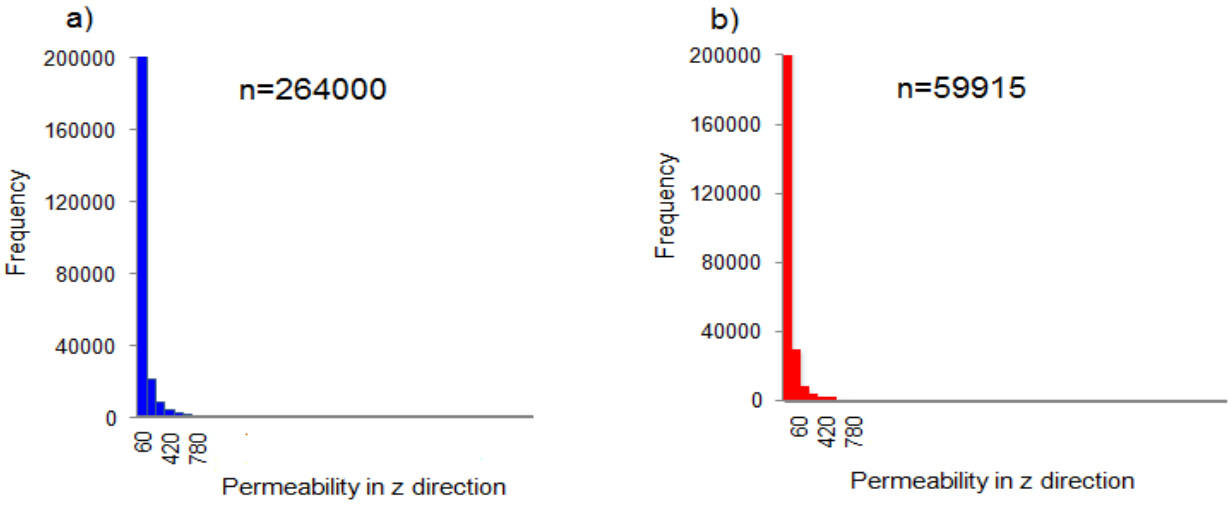

Figure 3.28. Comparison of permeability histograms in z direction in 20 - Layers Model for (a) Original model. (b) Coarse model (1).

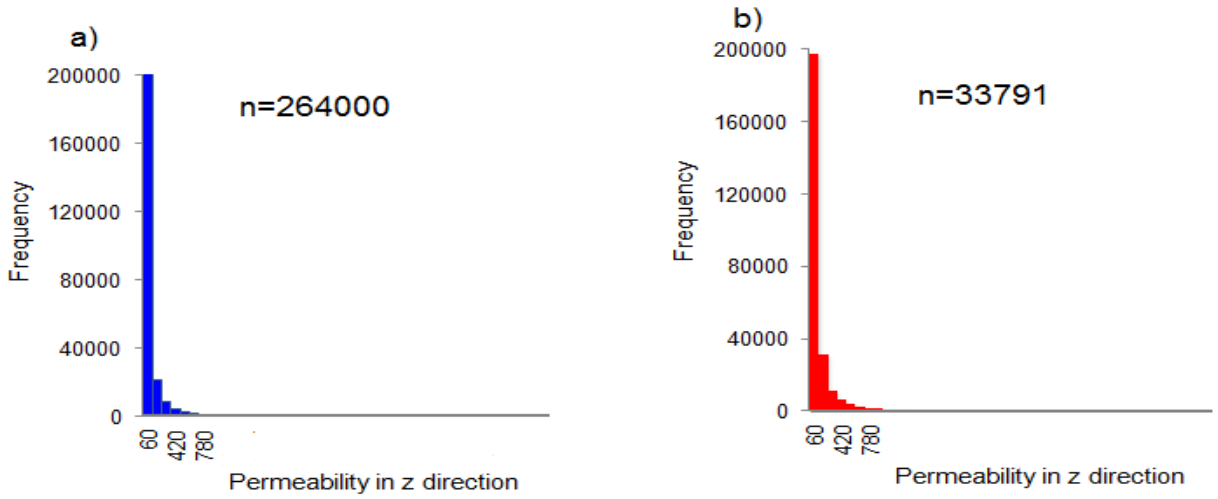

Figure 3.29. Comparison of permeability histograms in z direction in 20 - Layers Model for (a) Original model. (b) Coarse mode (2).

The Figure 3.30, Figure 3.31, Figure 3.32 and Figure 3.33 illustrate the results of simulations for the fine model and the coarse models (1) and (2).

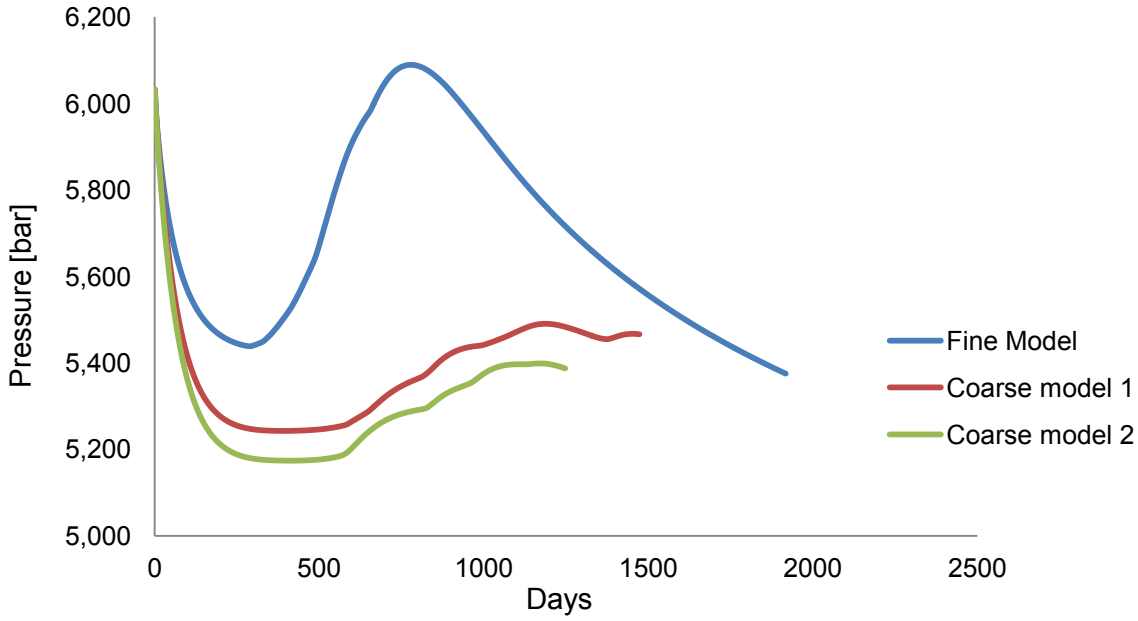

Figure 3.30. Comparison of field pressure for fine and coarse models (1) and (2).

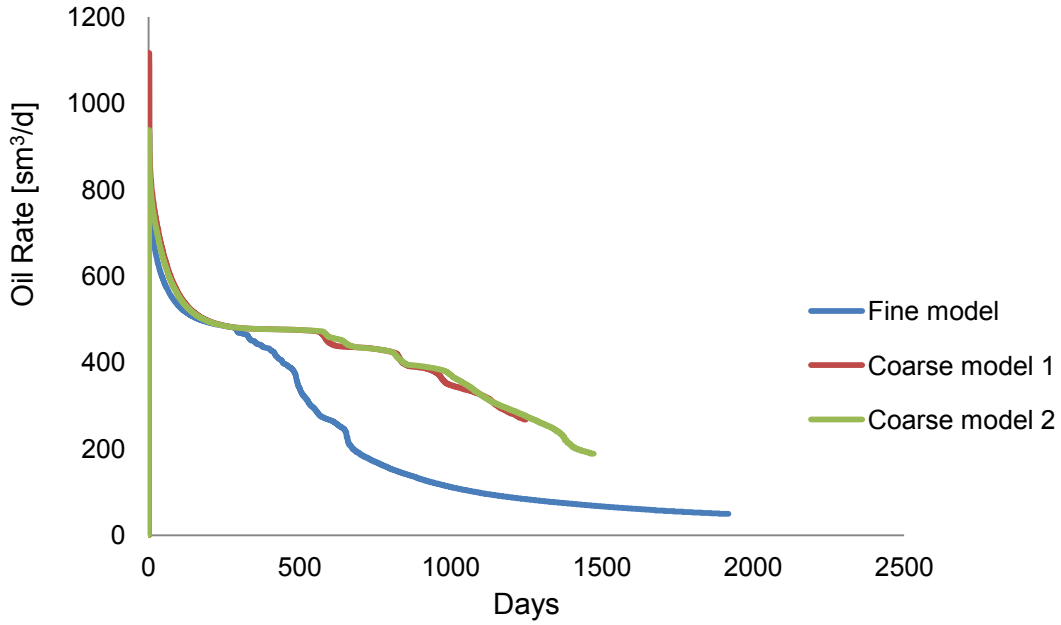

Figure 3.31. Comparison of field oil production for fine and coarse models (1) and (2).

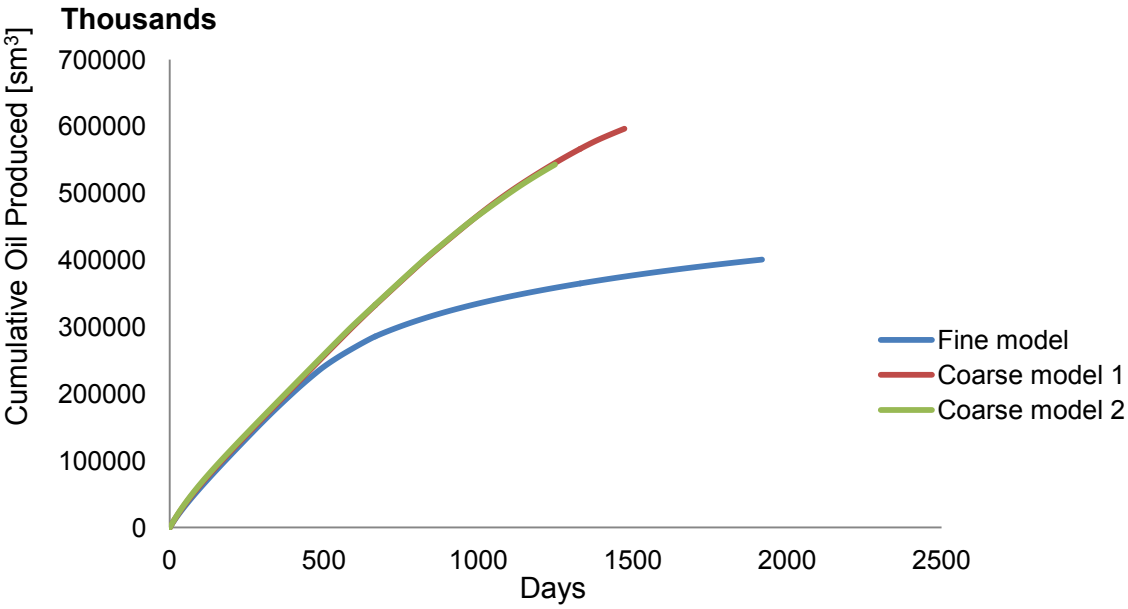

Figure 3.32. Comparison of field cumulative oil production for fine and coarse models (1) and (2).

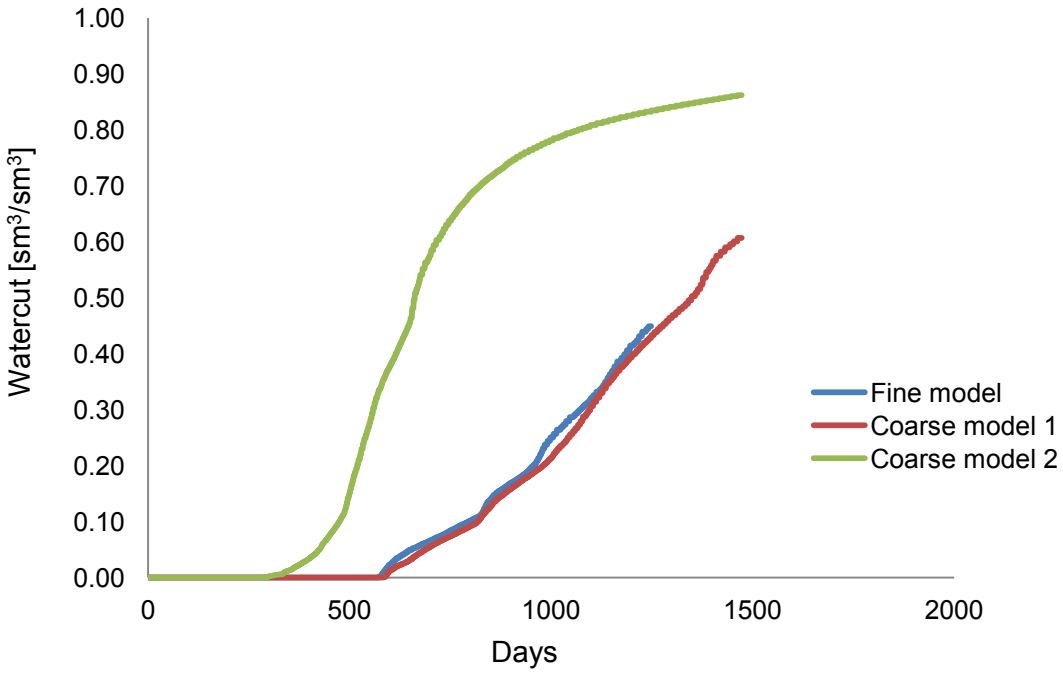

Figure 3.33. Comparison of field watercut for fine and coarse models (1) and (2).

In the second trial, the simulation is associated with a new strategy and new productivity index. Coarse models (3) and (4) contain properties, which are scaled up with two threshold numbers of 0.5 and 0.68. In the coarse model (3), the compression ratio and the number of grid cells for porosity are 0.07% and 263818. These values for Perm$x$ and Perm$z$ are obtained approximately 0.0, 264000 and 0.01%, 263979 respectively.

In the coarse model (4), the compression ratio and the number of grid cells for porosity are 74.34% and 67741. These values for Perm$x$ and Perm$z$ are obtained approximately 86.77%, 34925 and 86.72%, 35065 respectively.

Due to the similarity between the properties maps of the coarse model (3) with coarse model (1), only comparison of the coarse model (4) with the fine model are shown through Figure 3.34, Figure 3.35 , and Figure 3.36. Histograms in this step are similar to the previous step.

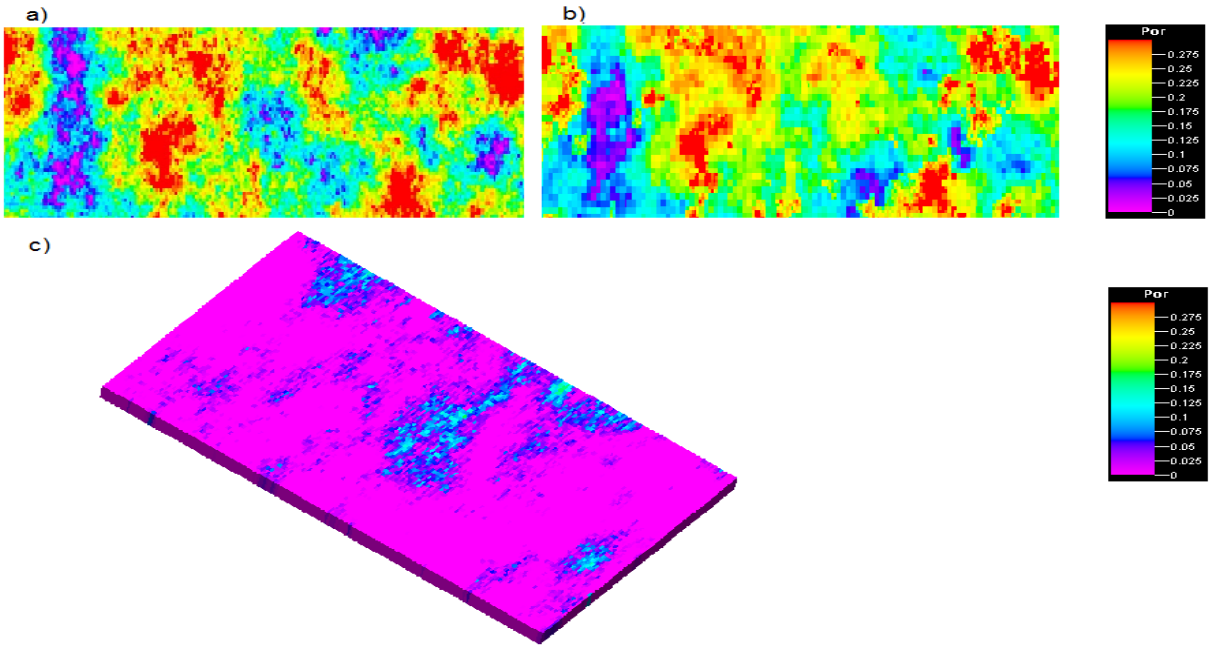

Figure 3.34. Comparison of porosity maps in 20 - Layers Model for (a) Original model. (b) Coarse model (4) upscaled to 264000 grid cells = 67741 grid cells and coarsening ratio 74.37%. (c) Difference between two maps (a) and (b).

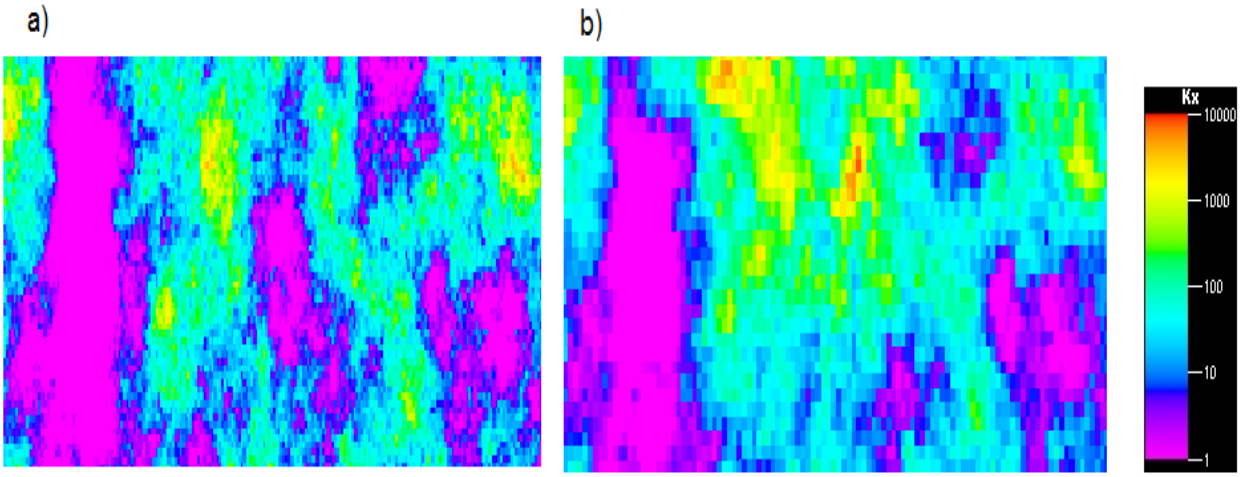

Figure 3.35. Comparison of permeability map in x direction in 20 - Layers Model for (a) Original model. (b) Coarse model (4) upscaled to 26400 grid cells = 34925 grid cells and coarsening ratio 86.77%.

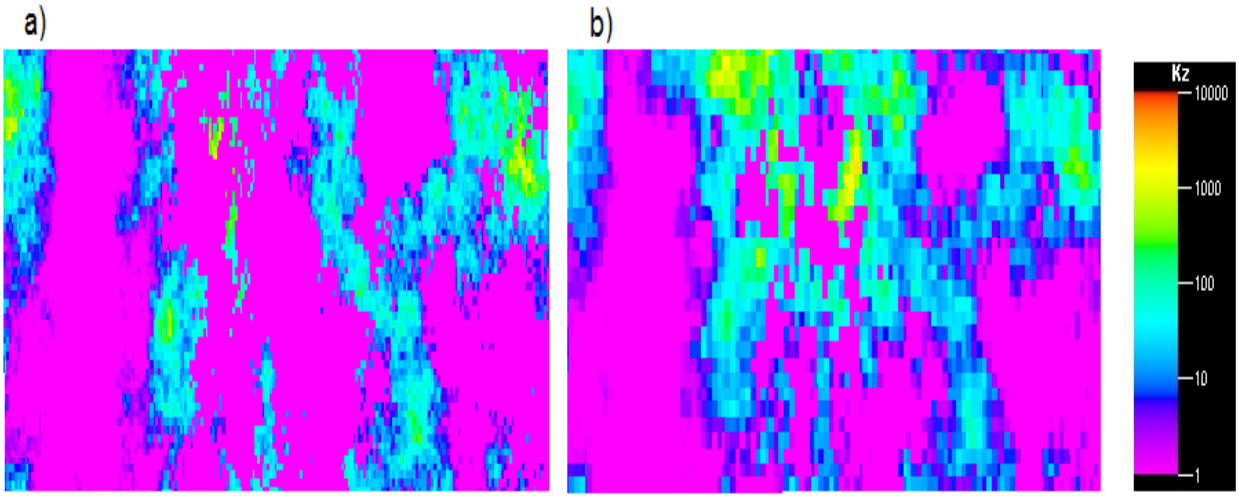

Figure 3.36. Comparison of permeability map in z direction in 20 - Layers Model for (a) Original model. (b) Coarse model (4) upscaled to 264000 grid cells = 35065 grid cells and coarsening ratio 86.72%.

Simulation results are illustrated through Figure 3.37 to Figure 3.40.

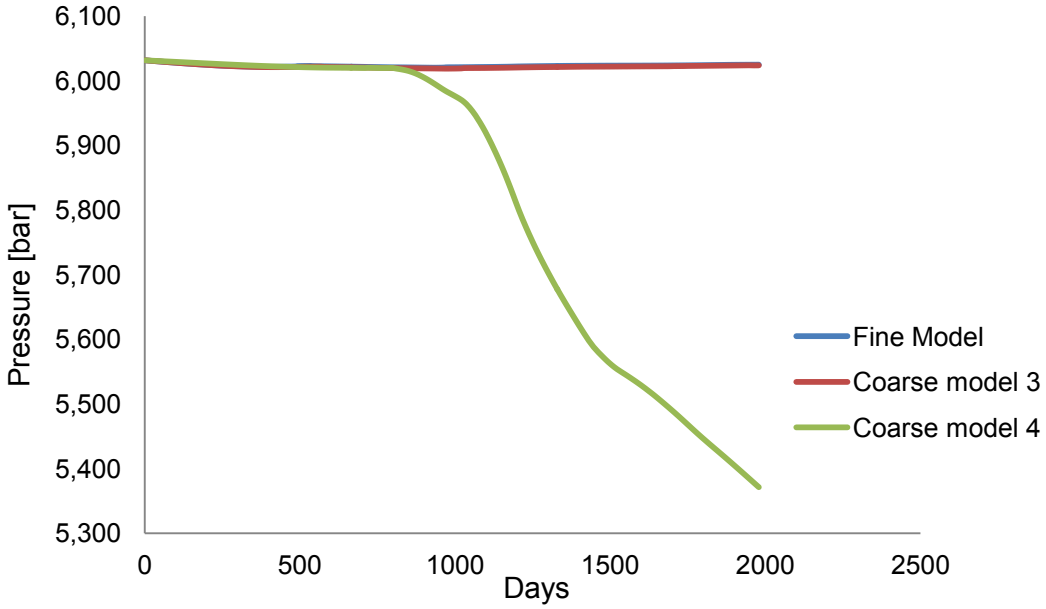

Figure 3.37. Comparison of field average pressure for fine and coarse models (3) and (4).

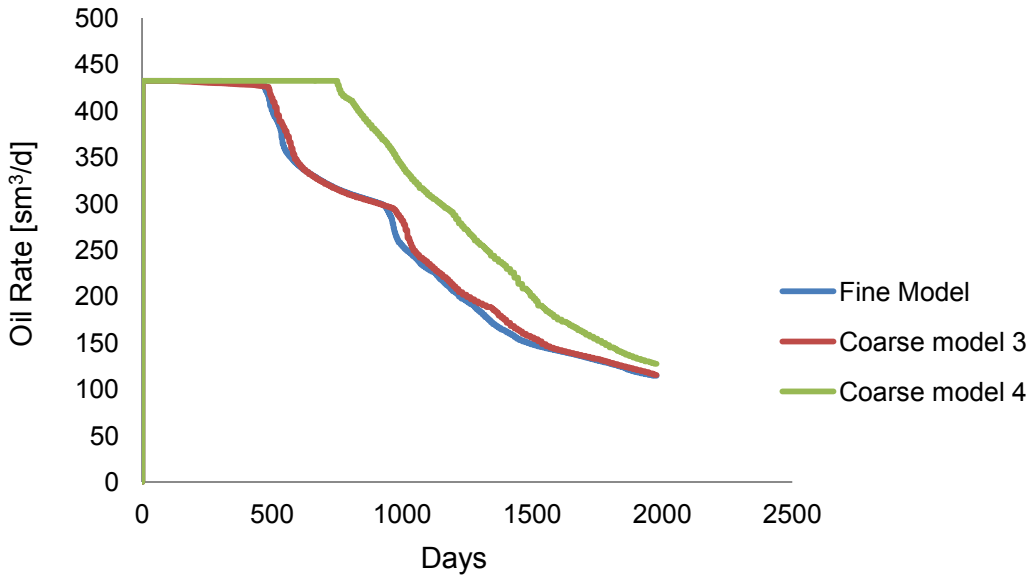

Figure 3.38. Comparison of field oil production for fine and coarse models (3) and (4).

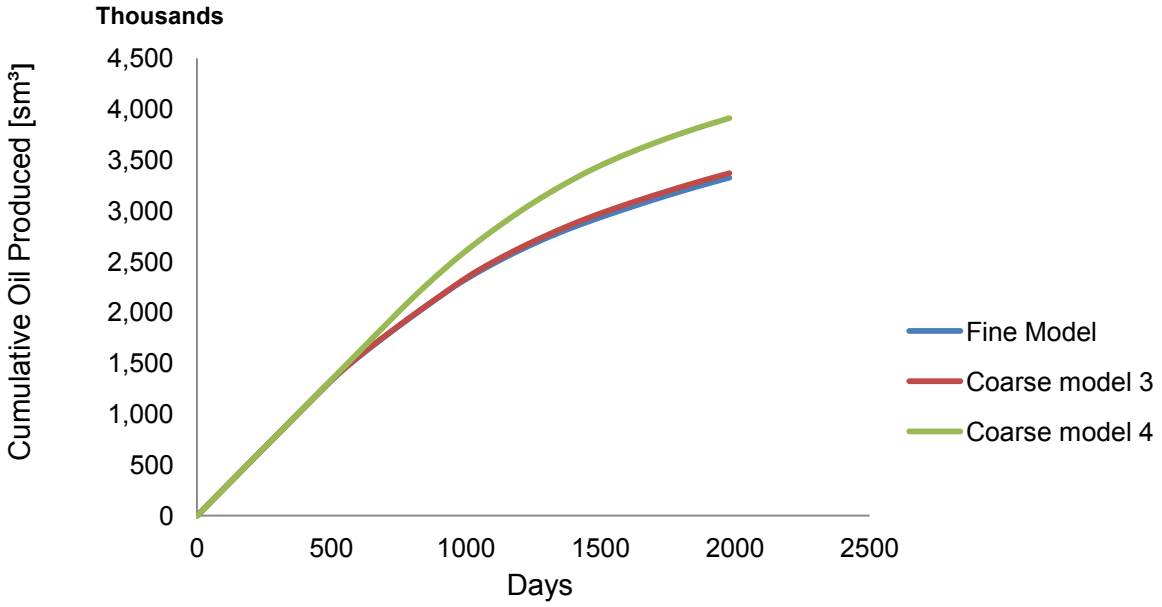

Figure 3.39. Comparison of field cumulative oil production for fine and coarse models (3) and (4).

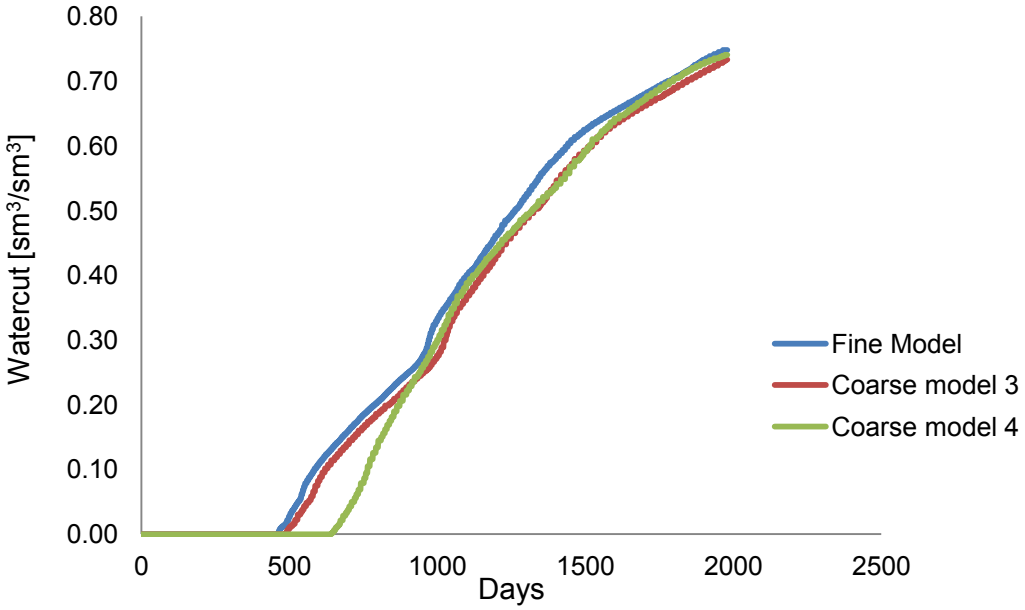

Figure 3.40. Comparison of field watercut for fine and coarse models (3) and (4).

In the third trial, the coarse models (5) and (6) include the simulation results of properties, which are scaled up layer by layer. In the coarse model (5), threshold number is considered 0.6 and the compression ratio and the number of grid cells for porosity are 26.44% and 194211. These values for Perm$x$ and Perm$z$ are obtained approximately 65.18%, 91917 and 61.73%, 101034 respectively.

In the coarse model (6), with threshold number 0.8, the compression ratio and the number of grid cells for porosity are 71.68% and 74778. These values for Perm$x$ and Perm$z$ are obtained approximately 74.63%, 66978 and 74.64%, 66957 respectively.

For a better comparison, the fine properties maps are compared again with the maps of these coarse models. Histograms of the coarse models are compared as well. Figure 3.41 to Figure 3.52 show the maps and their histograms.

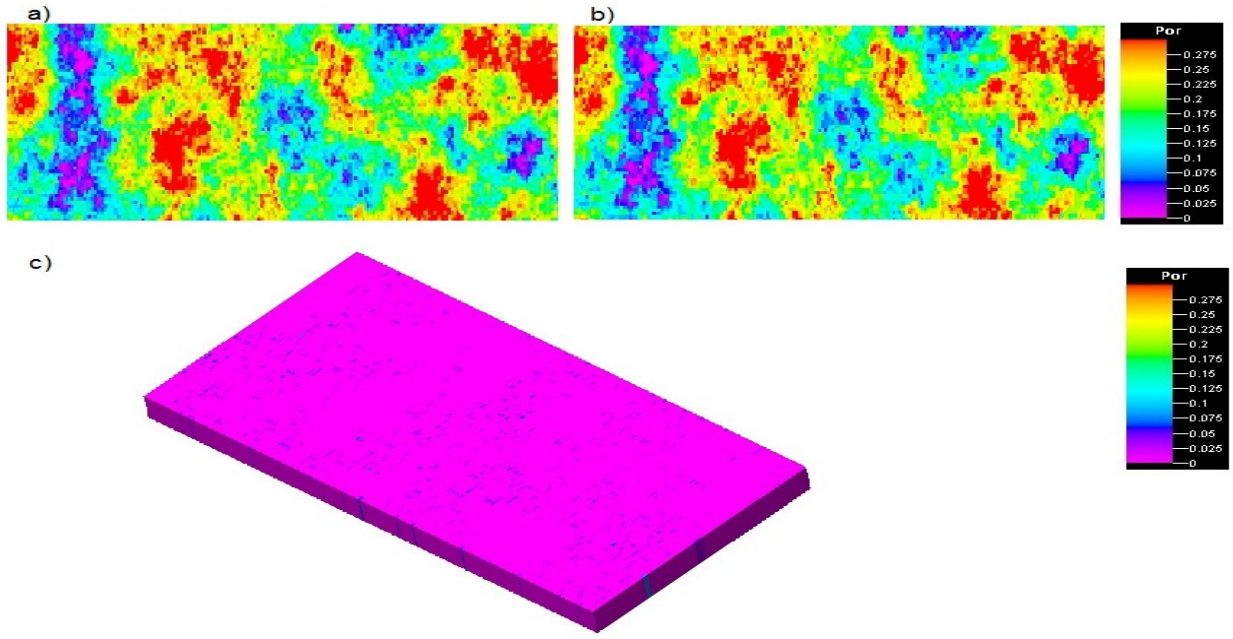

Figure 3.41. Comparison of porosity maps in 20 - Layers Model for (a) Original model. (b) Coarse model (5) upscaled to 264000 grid cells = 194211 grid cells and coarsening ratio 26.44%. (c) Difference between two maps (a) and (b).

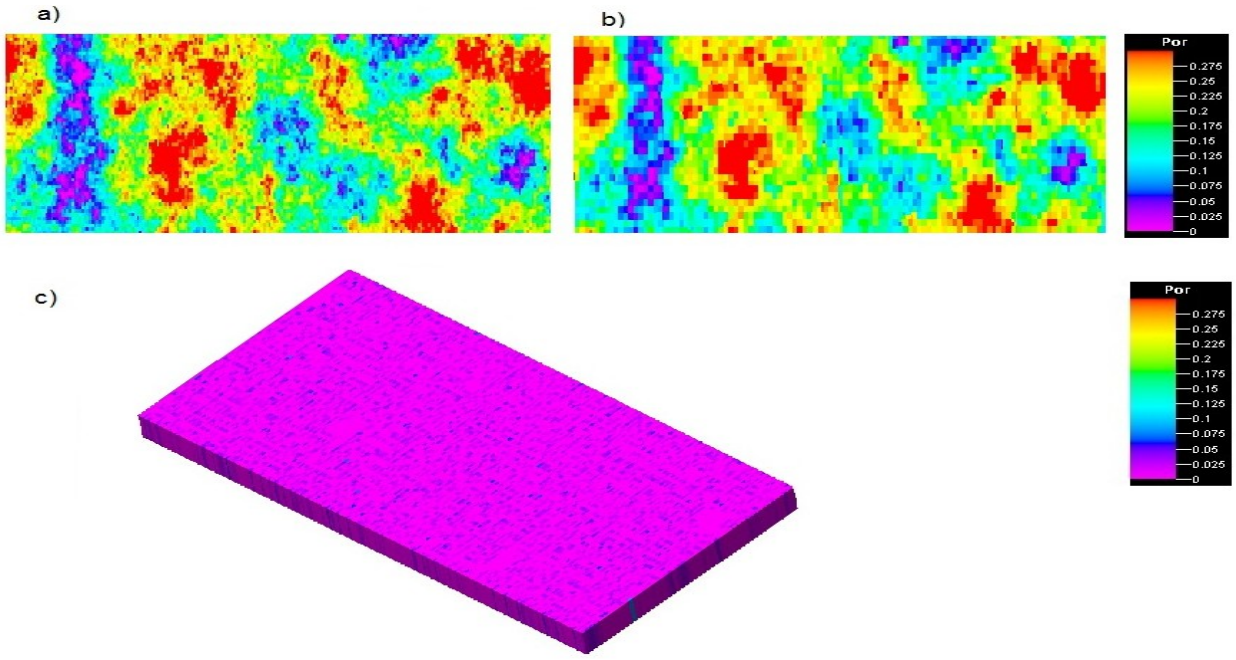

Figure 3.42. Comparison of porosity maps in 20 - Layers Model for (a) Original model. (b) Coarse model (6) upscaled to 26400 grid cells = 74788 grid cells and coarsening ratio 71.68%. (c) Difference between two maps (a) and (b).

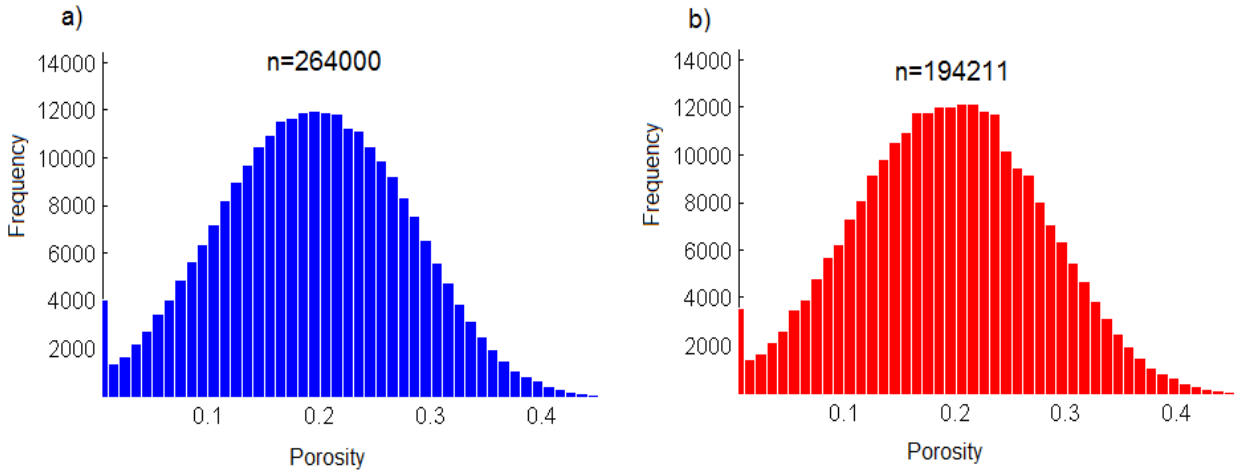

Figure 3.43. Comparison of porosity histograms in 20 - Layers Model for (a) Original model. (b) Coarse model (5).

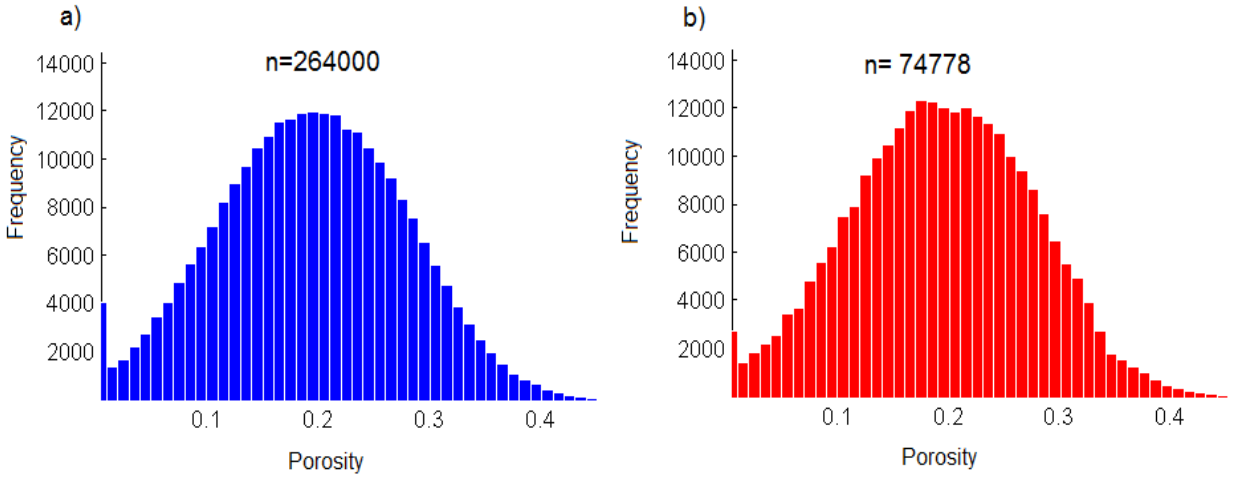

Figure 3.44. Comparison of porosity histograms in 20 - Layers Model for (a) Original model. (b) Coarse mode (6).

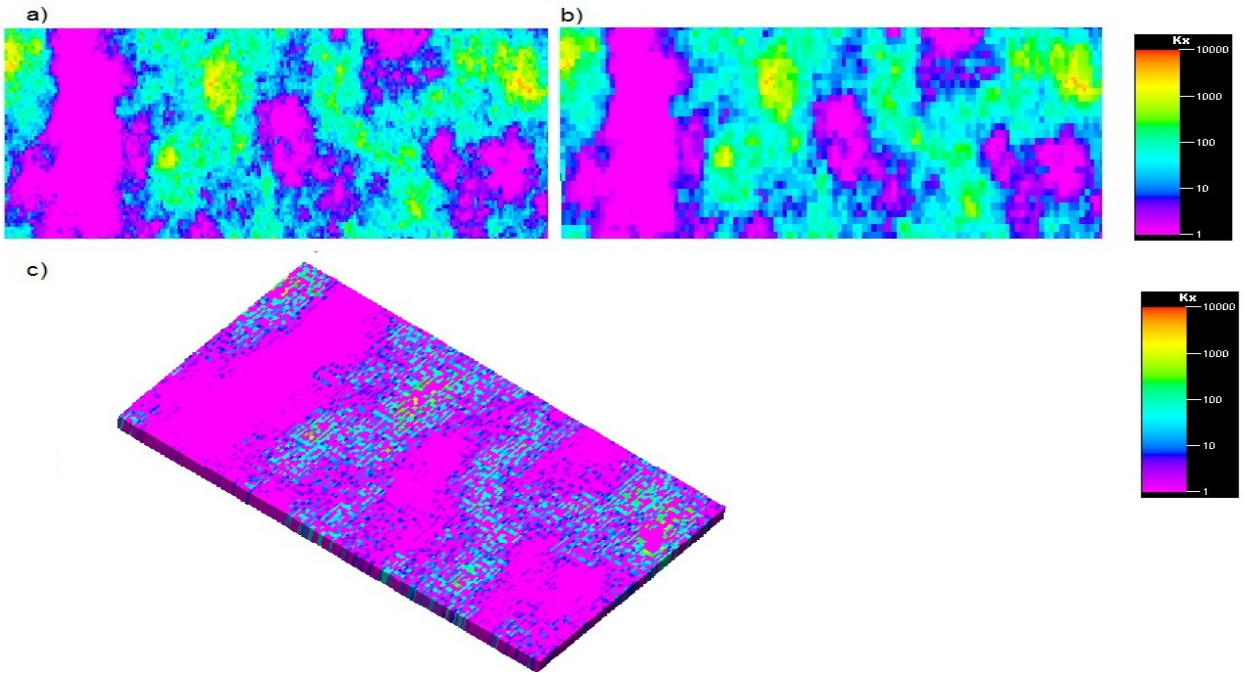

Figure 3.45. Comparison of permeability map in x direction in 20 - Layers Model for (a) Original model. (b) Coarse model (5) upscaled to 264000 grid cells = 91917 grid cells and coarsening ratio 65.18%. (c) Difference between two maps (a) and (b).

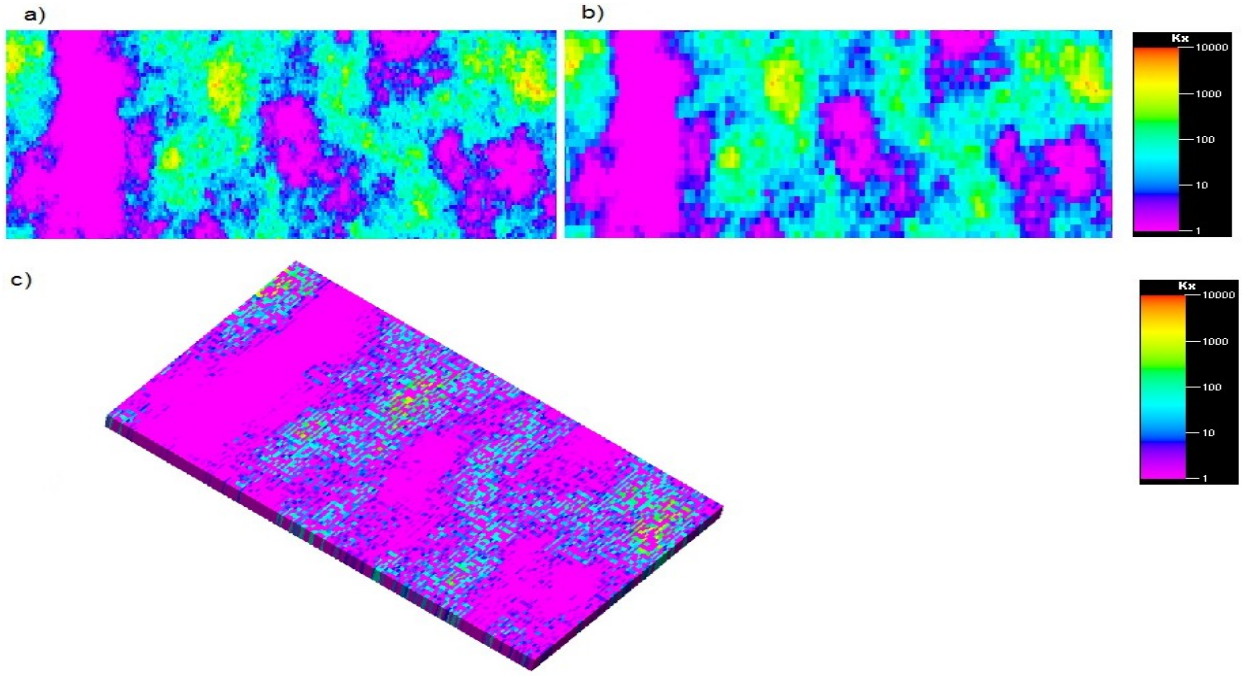

Figure 3.46. Comparison of permeability map in x direction in 20 - Layers Model for (a) Original model. (b) Coarse model (6) upscaled to 624000 grid cells = 66978 grid cells and coarsening ratio 74.63%. (c) Difference between two maps (a) and (b).

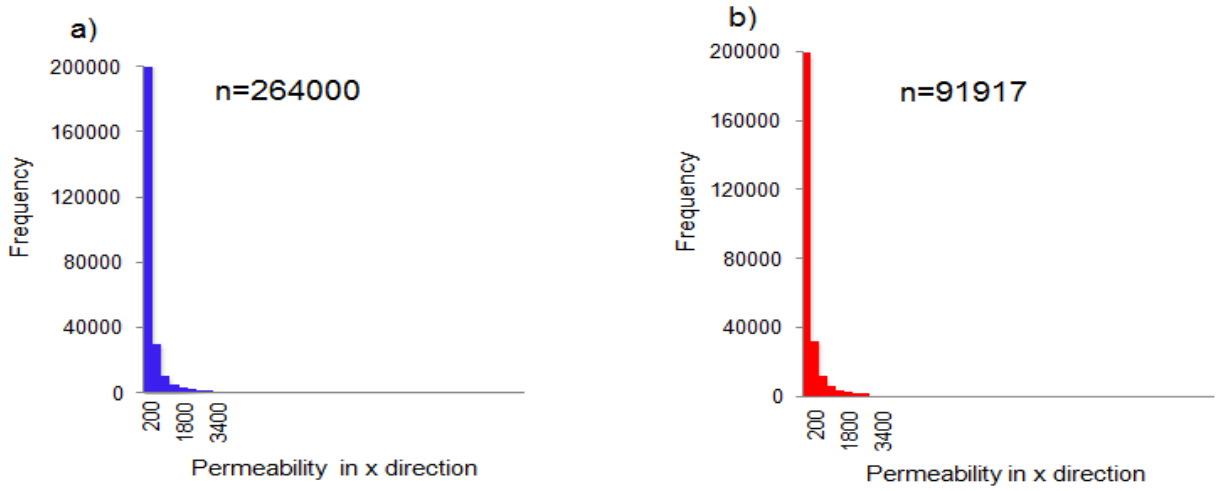

Figure 3.47. Comparison of permeability histograms in x direction in 20 - Layers Model for (a) Original model. (b) Coarse model (5).

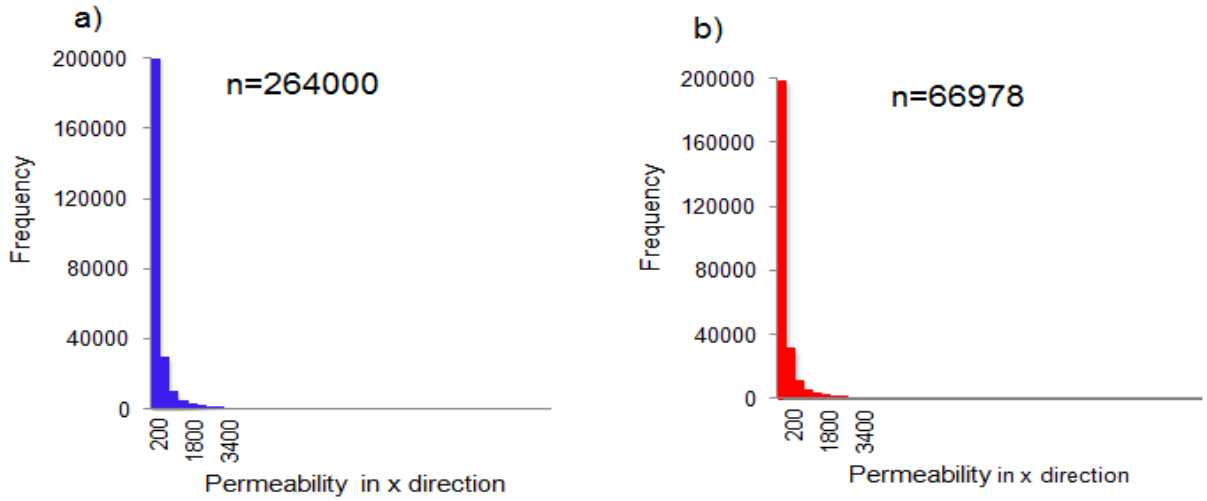

Figure 3.48. Comparison of permeability histograms in x direction in 20 - Layers Model for (a) Original model. (b) Coarse model (6).

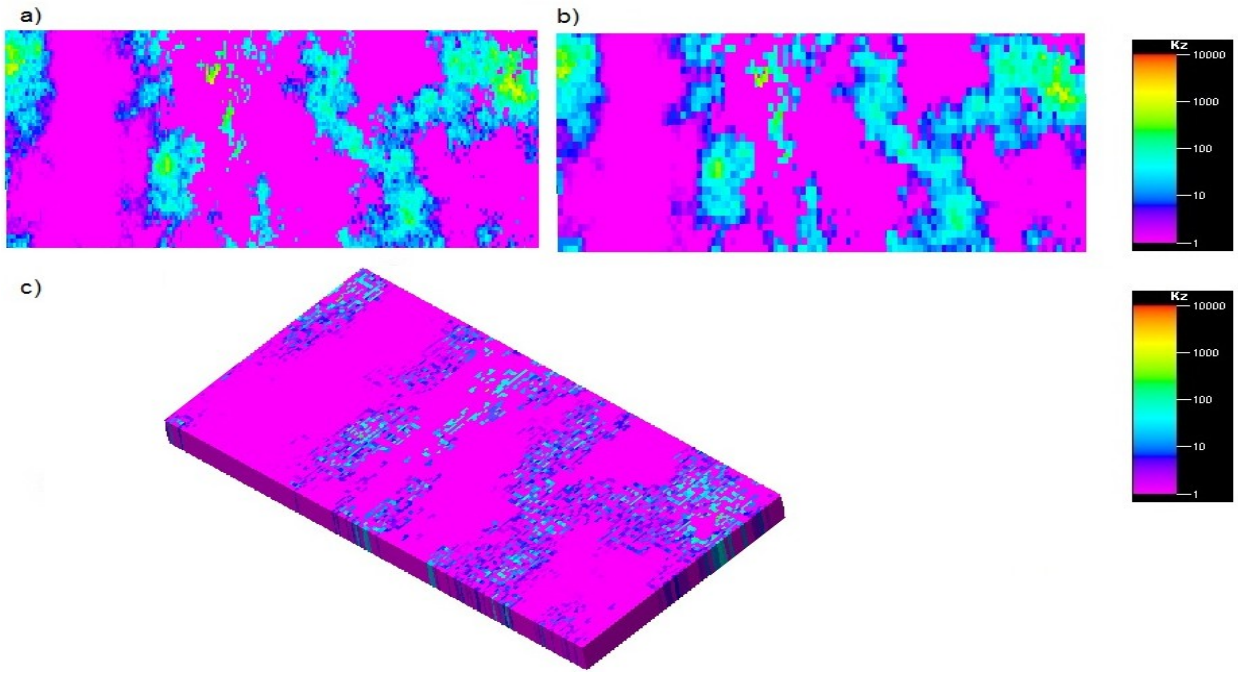

Figure 3.49. Comparison of permeability map in z direction in 20 - Layers Model for (a) Original model. (b) Coarse model (5) upscaled to 26400 grid cells = 101034 grid cells and coarsening ratio 61.73%. (c) Difference between two maps (a) and (b).

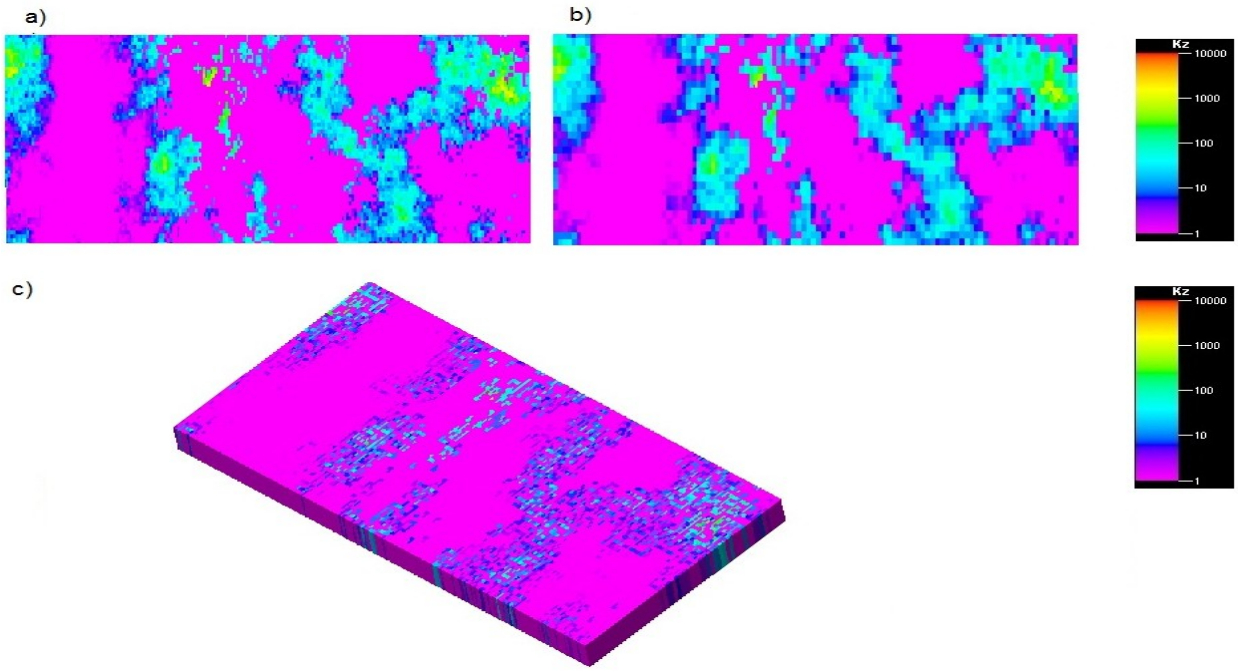

Figure 3.50. Comparison of permeability map in z direction in 20 - Layers Model for (a) Original model. (b) Coarse model (6) upscaled to 26400 grid cells = 66957 grid cells and coarsening ratio 74.64%. (c) Difference between two maps (a) and (b).

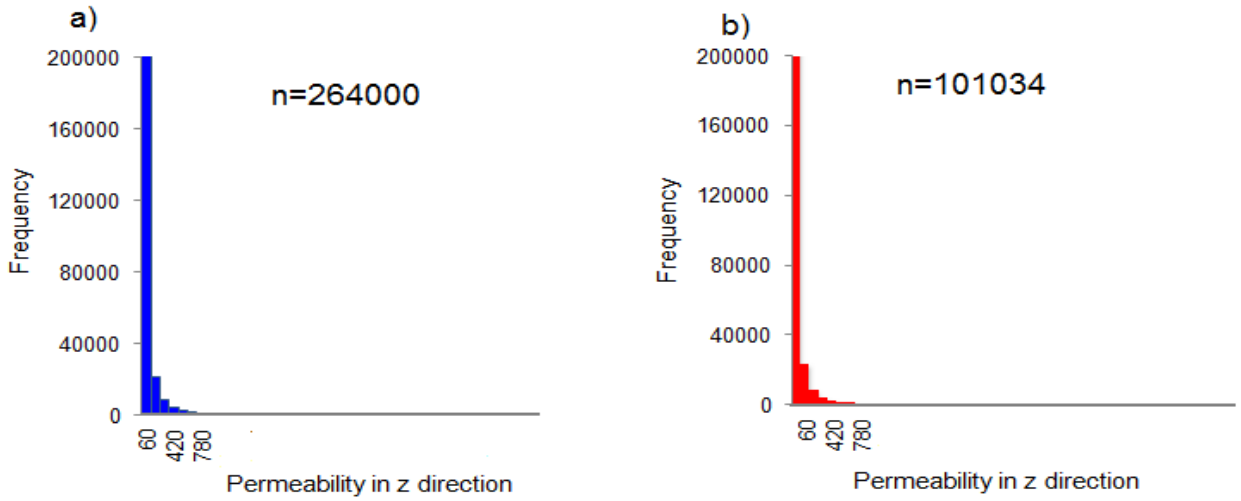

Figure 3.51. Comparison of permeability histograms in z direction in 20 - Layers Model for (a) Original model. (b) Coarse model (5).

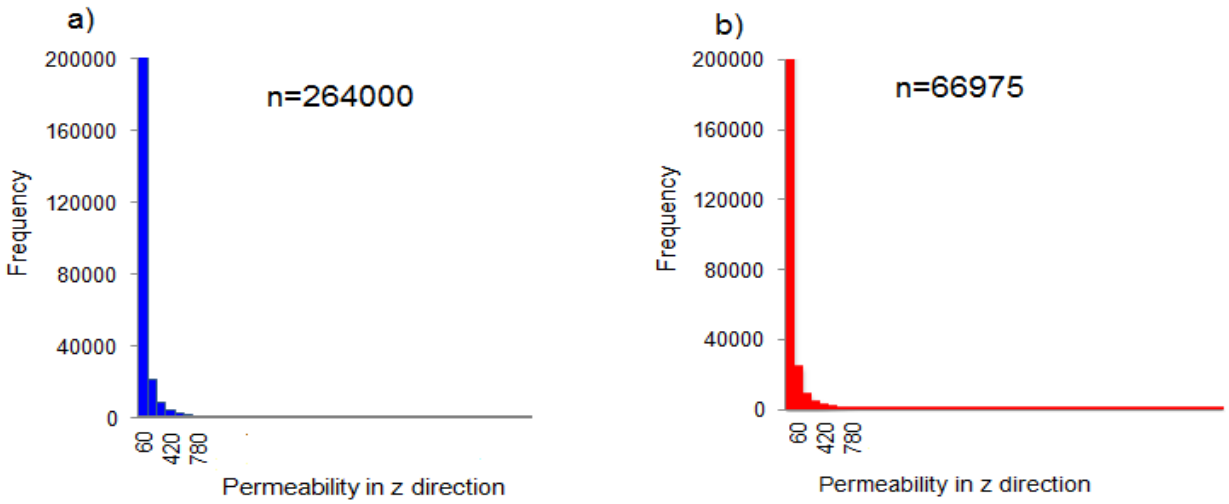

Figure 3.52. Comparison of permeability histograms in z direction in 20 - Layers Model for (a) Original model. (b) Coarse model (6).

The simulation results for the two coarse models (5) and (6) are illustrated through Figure 3.53 to Figure 3.56.

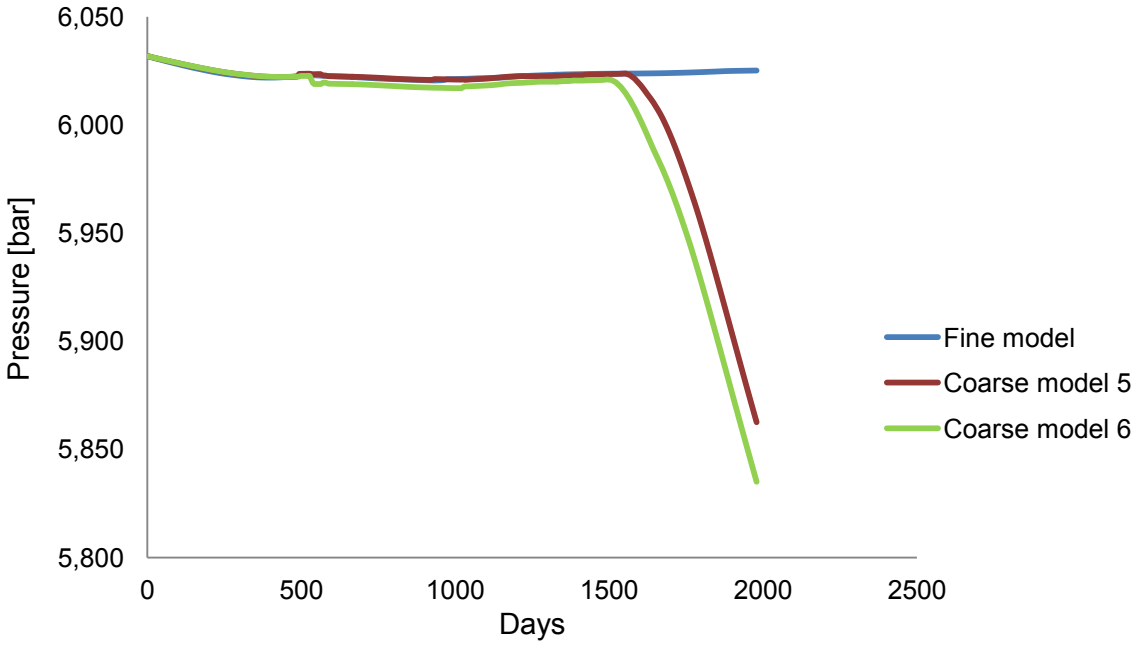

Figure 3.53. Comparison of field average pressure for fine and coarse models (5) and (6).

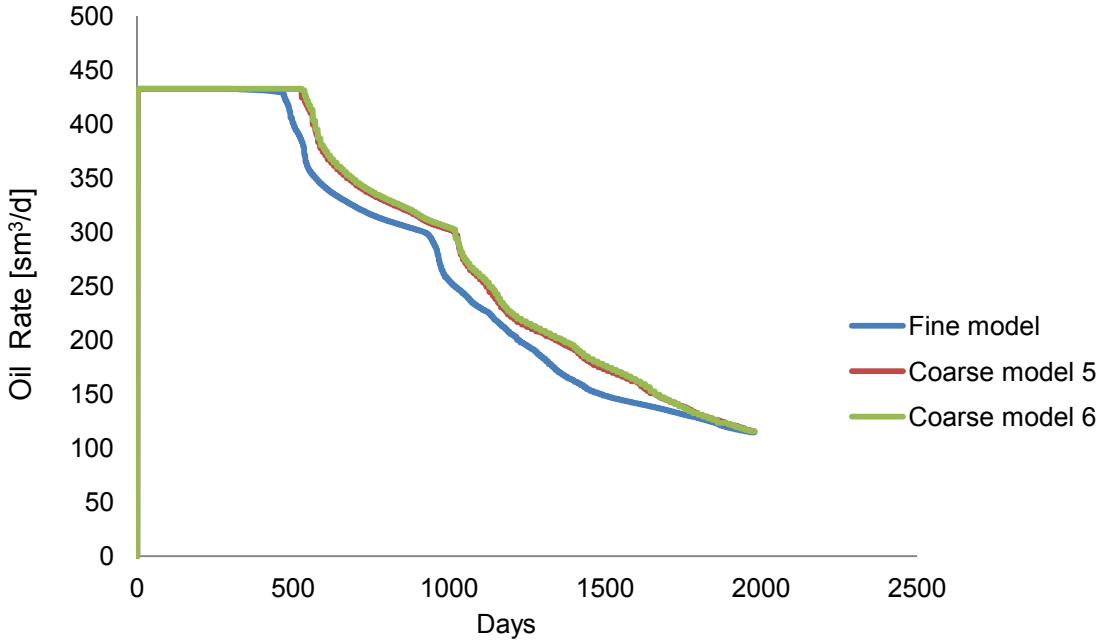

Figure 3.54. Comparison of field oil production for fine and coarse models (5) and (6).

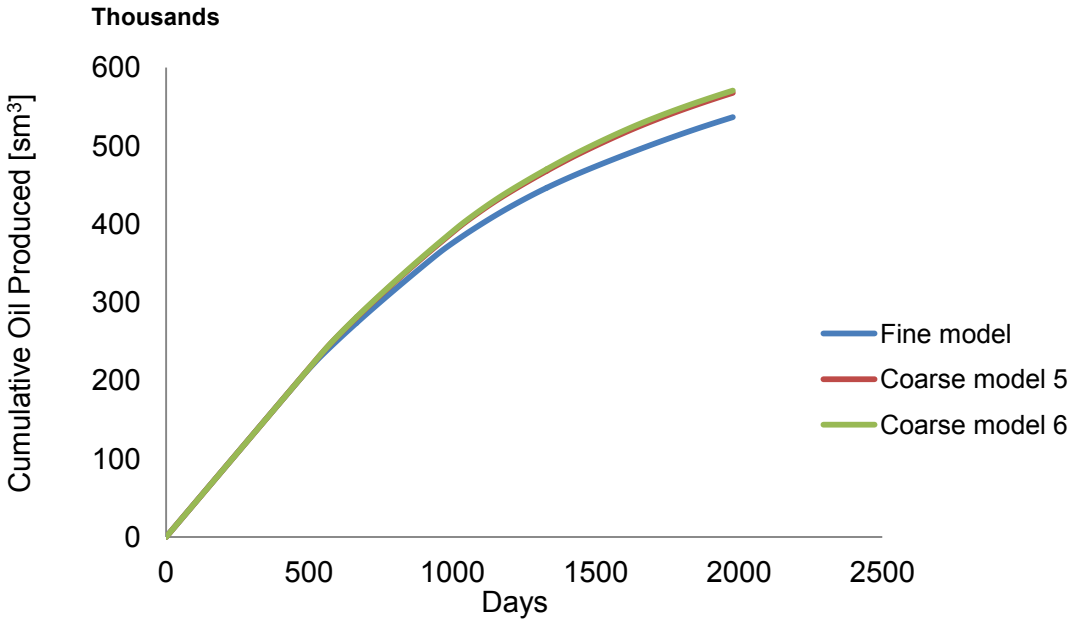

Figure 3.55. Comparison of field cumulative oil production for fine and coarse models (5) and (6).

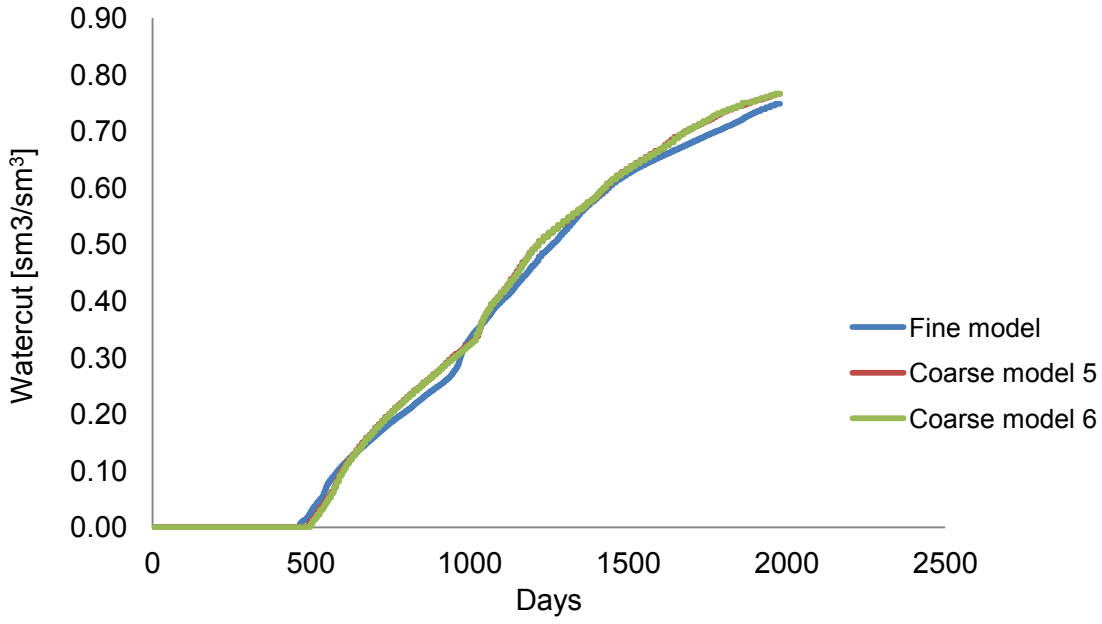

Figure 3.56. Comparison of field watercut for fine and coarse models (5) and (6).

As mentioned before, in the final step WCONPROD keyword in simulation software; Eclipse, is changed. This keyword is used to specify production control rate. For this step, the coarse models, (7) and (8) are defined. Similar to the previous procedure, the properties are scaled up with the threshold numbers 0.6 and 0.8.

Same as the coarse model (5), in the coarse model (7), threshold number is considered 0.6 and the compression ratio and the number of grid cells for porosity were 26.44% and 194211. These values for Perm$x$ and Perm$z$ are obtained approximately 65.18%, 91917 and 61.73%, 101034 respectively.

Moreover, same as the coarse model (6), in the coarse model (8), with the threshold number 0.8 the compression ratio and the number of grid cells for porosity were 71.68% and 74778. These values for Perm$x$ and Perm$z$ are obtained approximately 74.63%, 66978 and 74.64%, 66957 respectively. Figure 3.57 to Figure 3.60 illustrate the simulation results for this step.

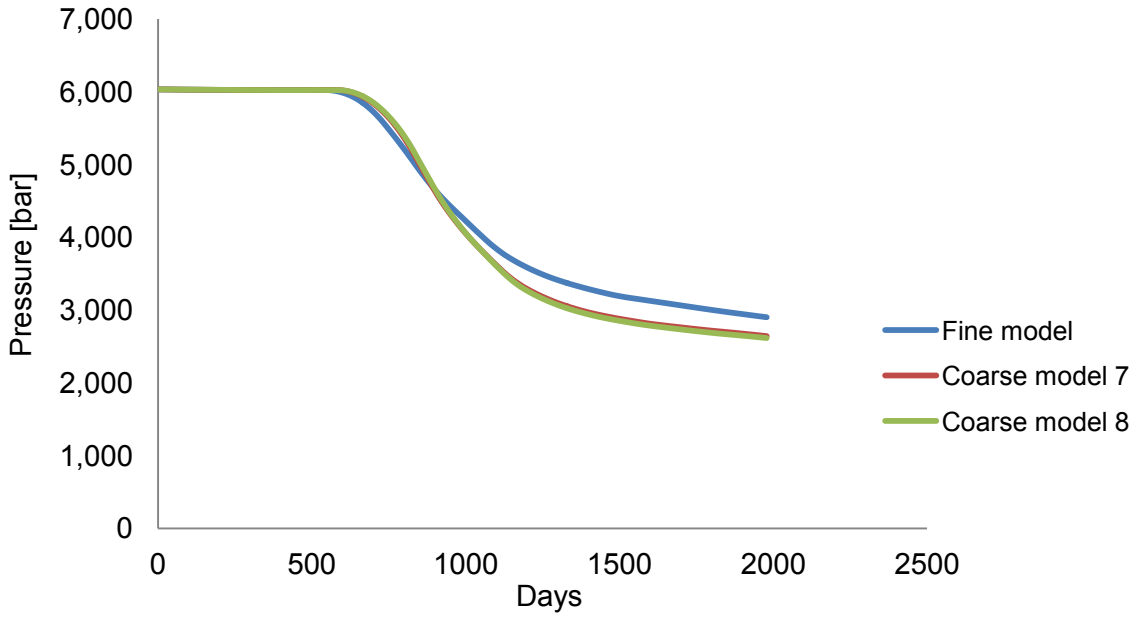

Figure 3.57. Comparison of field average pressure for fine and coarse models (7) and (8).

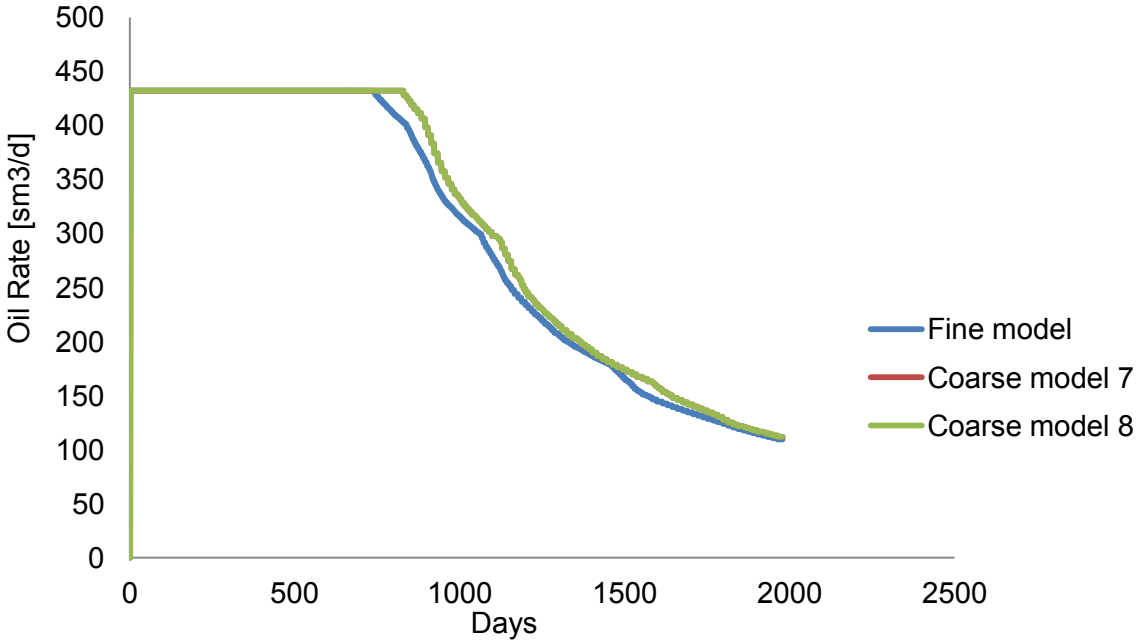

Figure 3.58. Comparison of field oil production for fine and coarse models (7) and (8).

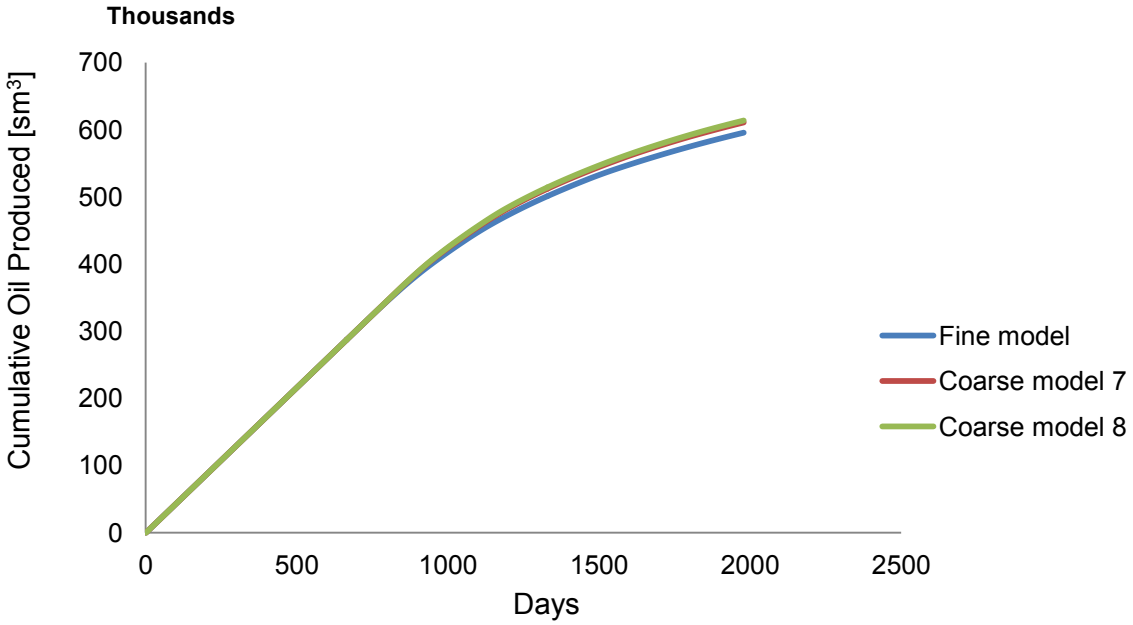

Figure 3.59. Comparison of field cumulative oil production for fine and coarse models (7) and (8).

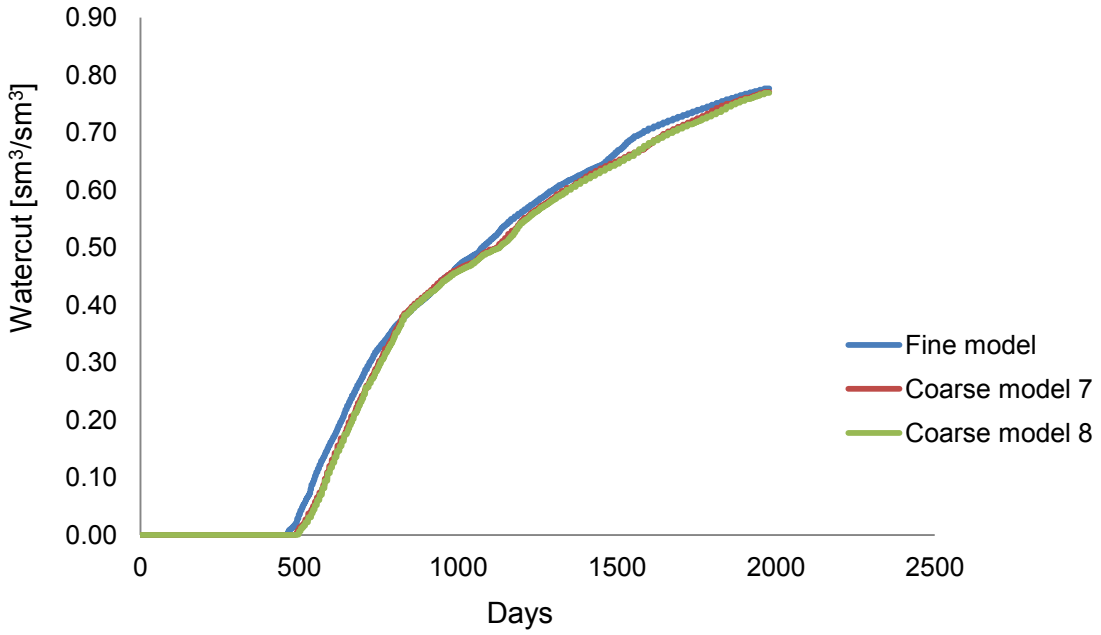

Figure 3.60. Comparison of field watercut for fine and coarse models (7) and (8).

At the end of this section, the final elapsed CPU and time to run the simulated fine and coarse models are reported in Table 3.2. Comparison of final CPU and Time elapsed for fine and coarse models (7) and (8).. Pore volume for these cases are also calculated and reported. Comparison of OIP between three discussed models of trial (4) is illustrated through Figure 3.61. Comparison between pore volumes changes is shown in Table 3.3.

Table 3.2. Comparison of final CPU and Time elapsed for fine and coarse models (7) and (8).

Final elapsed CPU for the fine model	27654.45
Final elapsed CPU for the coarse model (7)	26828.72
Final elapsed CPU for the coarse model (8)	20730.56
Elapsed time for the fine model	more than 8hours
Elapsed time for running the coarse model (7)	less than 8 hours
Elapsed time for running the coarse model (8)	less than 6 hours

Table 3.3. Comparison of pore volumes for fine and 3D coarse models.

Pore volume for 3D model 20-Layers [rm^3]	Difference between fine and coarse model (7) (%)	Difference between fine and coarse model (8) (%)
	0.000032	0.000065

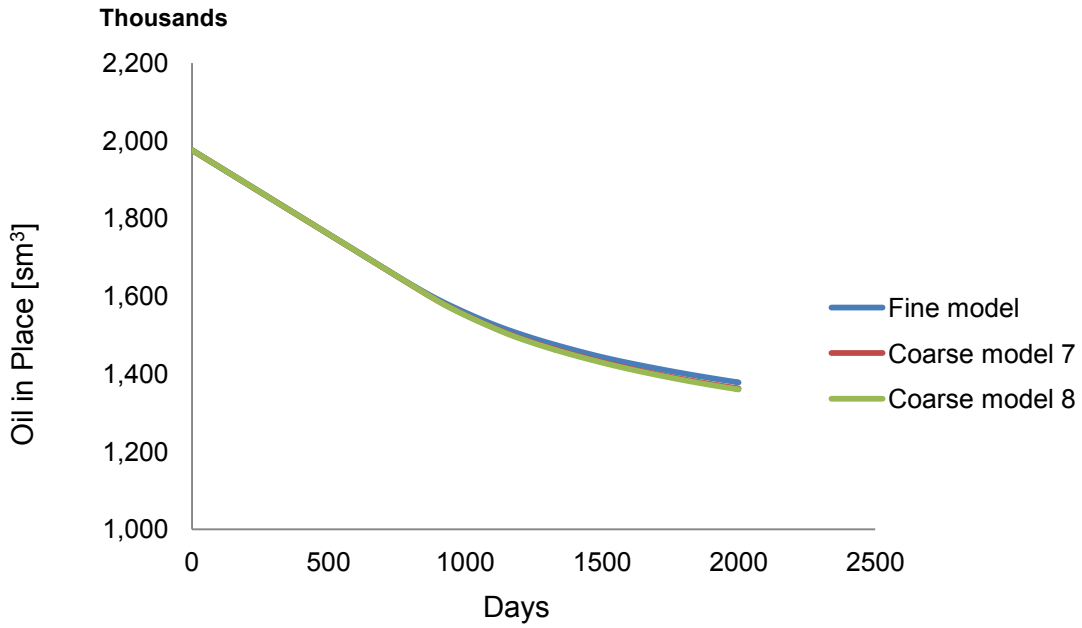

Figure 3.61. Comparison of OIP for fine and coarse models (7) and (8).

Based on the description of the previous section, the fine geological model scale in our study is described on a regular Cartesian grid. It has 60 x 220 x 85 cells (1,122,000cells) and it is a full original SPE'10 model.

In this step, properties are scalded up with threshold number 0.8 and the simulation results of both the fine and the coarse model are compared with two upscaled models by the Chevron and TotalFinaElf simulators, which were presented in SPE 10 paper.

The number of grids after upscaling for porosity, perm$x$, and perm$z$ are 319871, 283493 and 282986 respectively. The simulation results for field average pressure, oil production rate, cumulative oil production, and water cut of the producer 1 like the

paper for the fine and the coarse models are compared through Figure 3.62 to Figure 3.65. Comparison of OIP between both the fine and the coarse model WT is illustrated through Figure 3.66.

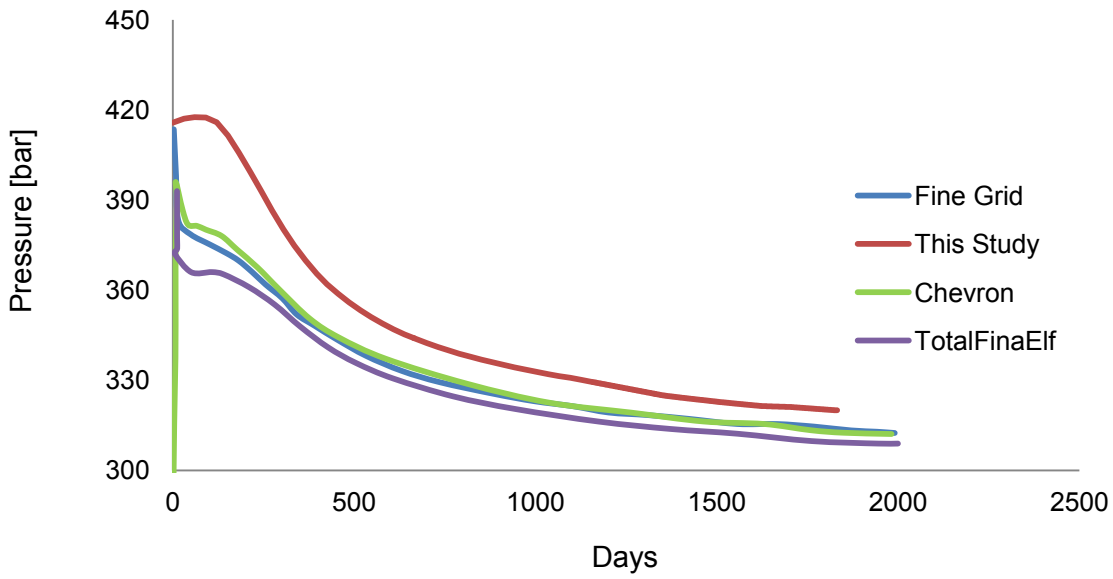

Figure 3.62. Comparison of field average pressure for fine and coarse models.

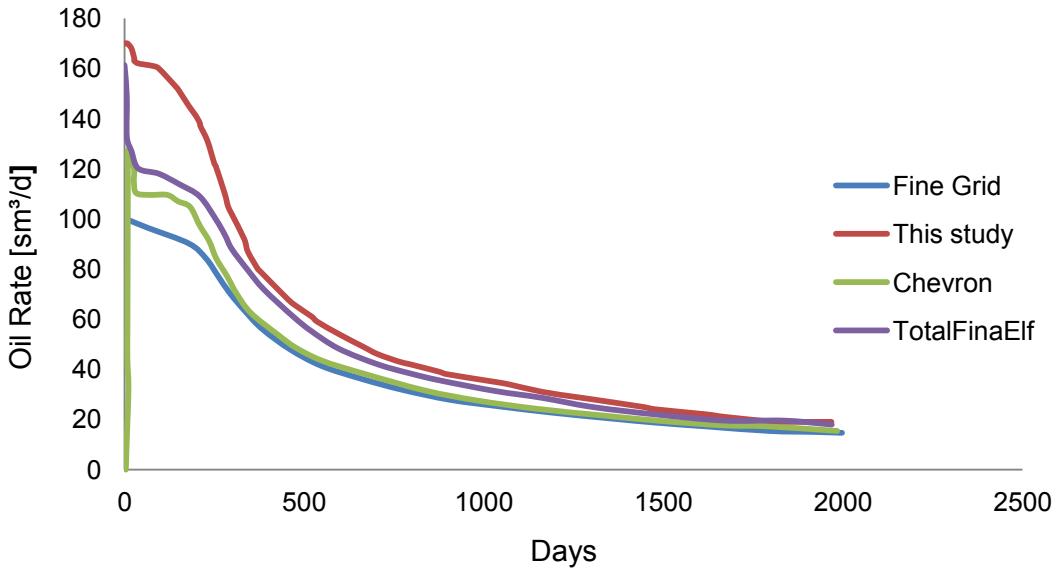

Figure 3.63. Comparison of producer 1 oil production for fine and coarse models.

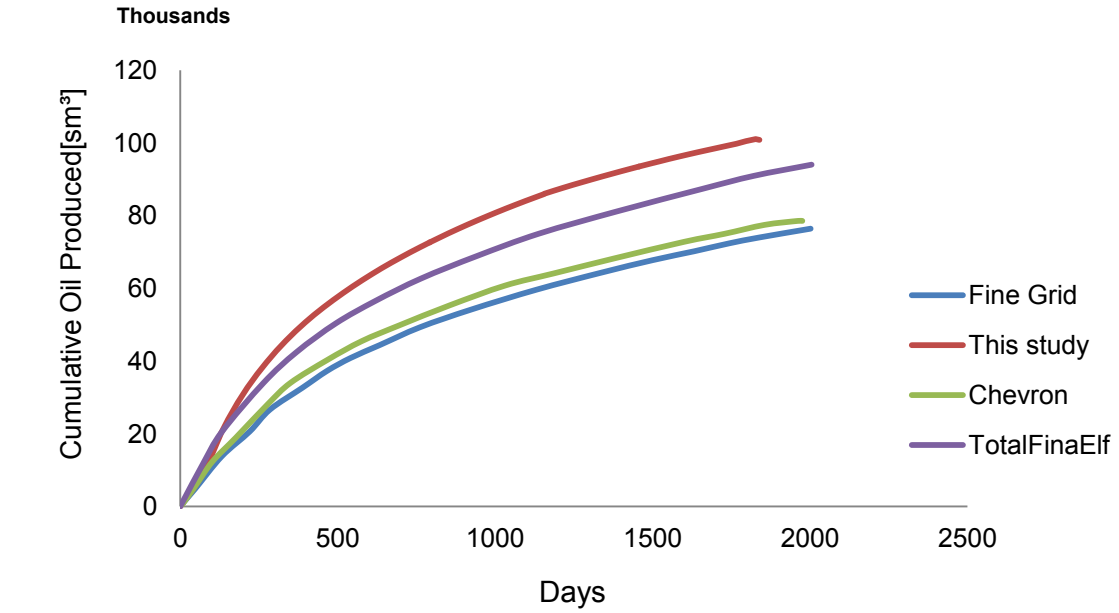

Figure 3.64. Comparison of producer 1 cumulative oil production for fine and coarse models.

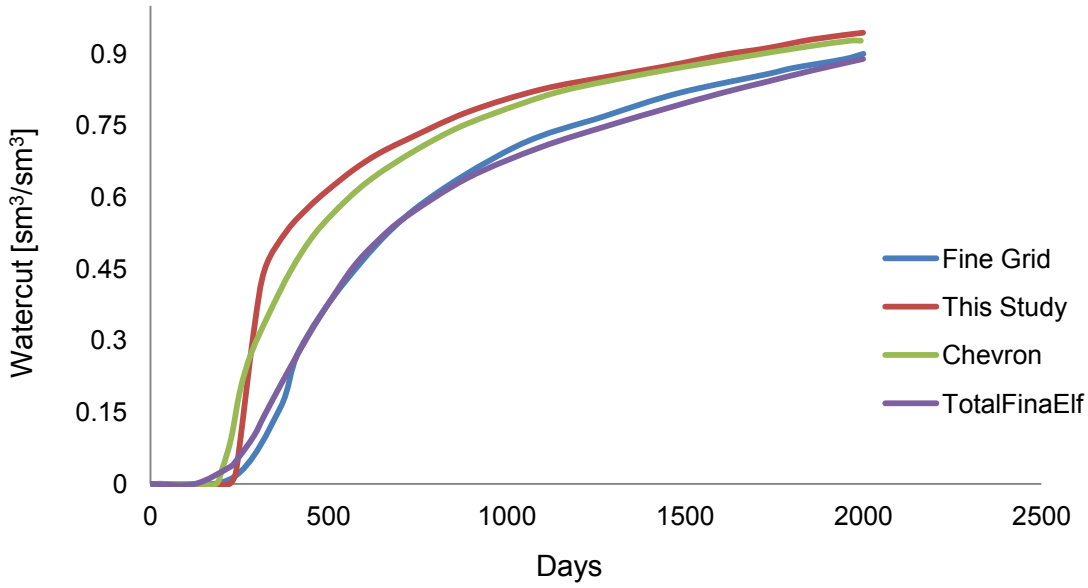

Figure 3.65. Comparison of producer 1 watercut for fine and coarse models.

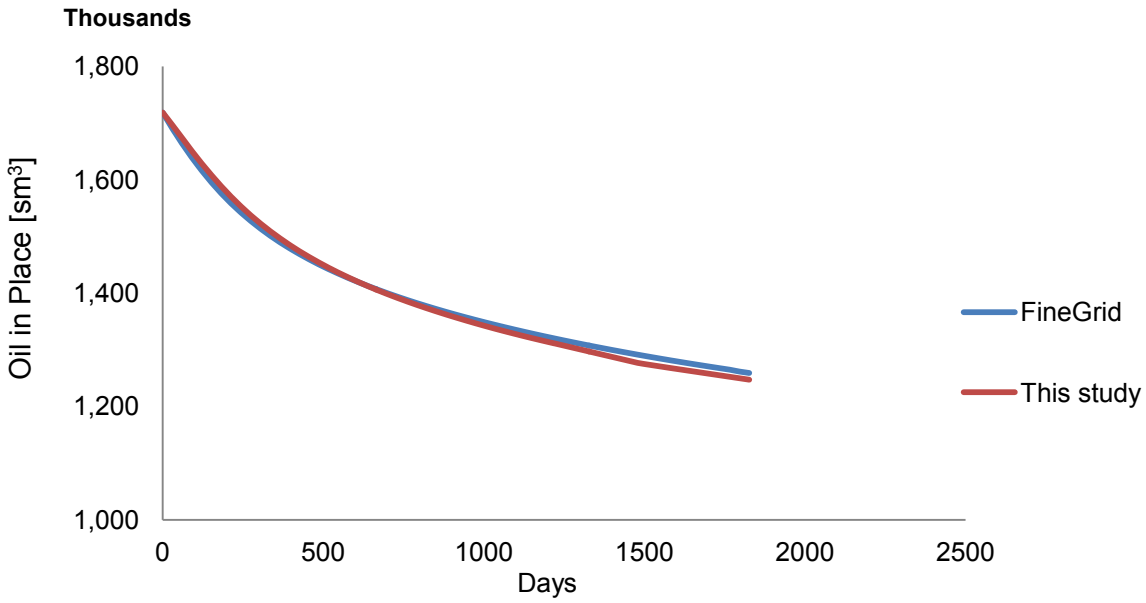

Figure 3.66. Comparison of OIP for fine and coarse models.

4 Discussion

The presented results are discussed accordance with 2D upscaling and 3D upscaling.

4.1 2D Upscaling

Based on the results as shown in the figures above, the upscaled properties and their histograms in each level of upscaling are compared visually to their corresponding fine properties through Figure 3.1, to Figure 3.12. As you see in the mentioned figures, the coarsening ratio in the second level is higher and the numbers of girds are less than its first level. The reasons for these differences refer to the WT transformation algorithm. In the second level, every eight cells of the fine model are upscaled to make one cell in the coarse model while in the first level; every four cells are combined to create one cell in the upscaled model.

The histograms show the property distributions for each level. In both levels of upscaling, porosity is distributed wider than perm x and perm z and its frequency is less than before. Due to the wide distribution of porosity in this study, also due to the WT algorithm, the upscaling process is performed firstly by porosity and then by permeability in both x and z direction.

The simulation results show that 2D upscaling meet the expected outcomes very well. Field pressure, field production oil rate, field cumulative oil production and water cut diagrams were illustrated through Figure 3.3 to Figure 3.16, which give the best results of upscaling for both; first and second levels. **Figure 3.13** shows the pressure changes in the presence of injectors and producers. As it can be seen, there is small deviation between the fine and the coarse model of the second level, which can be referred to definition of development simulation strategy, but this deviation could be negligible. Figure 3.17 represents the comparison of OIP between three models. No any difference observed in this diagram show that the applying of upscaling on this parameter is ineffective. The differences between pore volume of the fine and both of coarse models, presented in Table 3.1 show that the upscaling effect on the fine model in term of pore volume is very small and negligible.

4.2 3D Upscaling

To discuss 3D upscaling, along with those parameters, which have been investigated in 2D upscaling, CPU, time and capacity storage for running the model are considered as well. 3D model in comparison with 2D model is more much larger, hence some issues such as time and capacity are affected in order to run the model. In other hand, due to the large volume of this model, more time and RAM are elapsed. As mentioned in the previous section, the final CPU, and the elapsed time to run the upscaled models were less than the corresponding time to run the fine model.

4.2.1 20 layers

In this part, the obtained results are investigated with different threshold numbers. According to the diagrams represented above, after many trial and errors, four cases have been chosen to investigate the performance of WT in 3D upscaling and for 20 layers.

- **First Trial: Fine model and coarse model (1) and (2)**

In this step, the results obtained from the mentioned cases are compared together. Figure 3.18 to Figure 3.19, Figure 3.22 to Figure 3.23 and Figure 3.26 to Figure 3.27 show the comparison of properties maps of fine and coarse models (1) and (2).

These maps give us relative satisfactory results based on the WT transformation algorithm. As it can be seen in Figure 3.19, Figure 3.23 and Figure 3.27, the effect of higher coarsening ratio on properties is comparable to the lower ratio. In the other hand, threshold number 0.8 provided larger grid cells for all properties. Because the number of grids, which are coarsened in coarse model (1), are less than the other case and the similarity between the maps of the fine and the coarse model (1) emphasizes this matter. The histograms for all mentioned cases in the Figure 3.20, Figure 3.21, Figure 3.24, Figure 3.25, Figure 3.28 and Figure 3.29 represent the distribution of the properties. Similar to the 2D upscaling, porosity histogram is distributed wider than to other properties and it has less frequency. In the first trial, I could not get conclusive simulation results (Figure 3.30 to Figure 3.33) even for the coarse model (1). Despite the similarity of these case maps with the fine maps, there

are big deviations between their simulation results. One reason refers to the scenarios that were defined for the simulation. It was not appropriate to meet the expected outcomes.

- **Second Trial**: **Fine model and coarse models (3) and (4)**

To improve the performance of upscaling in this step the essential parameters for simulation are changed. In addition, new productivity index is added to the scenario as it was pointed out above. Due to similarity between the properties maps of the coarse model (3) and the fine model, and also their histograms, only the properties maps of the coarse model (4) are shown through Figure 3.34, Figure 3.35,Figure 3.36, As it can be seen, percentage of threshold number 0.68 provides properties maps with larger coarsened grids. The simulation outputs, as illustrated in Figure 3.37 to Figure 3.40, are different from the last step results. In the previous step, although there are deviations between the simulations charts, a harmony is observed between them. In other words, the diagrams change in the same direction and the fine model results are closed to the coarse model (3) except in pressure.

- **Third Trial: Fine model and coarse model (5) and (6)**

The deviations mentioned in the last trial show, that there is still a problem and something has to be reviewed again. This time the properties are scaled up layer by layer. Properties maps of the fine model and the coarse models (5) and (6) and also their histograms compared through Figure 3.41 to Figure 3.52. Since the lower value of case (5); 0.6 is chosen higher than its corresponding value in the previous trials; 0.5, there is not similarity between its properties maps with the fine model or in other hand in this case, properties are coarsened more than previous one. To run the simulation, the discussed parameters have not been changed. The results are represented in Figure 3.53 to Figure 3.56. The new obtained outcomes except pressure looked better than the previous one. There are still small differences between the two models with the fine model. However, it is a good sign to change some parameters to get desired results.

❖ **Fourth Trial: Fine model and coarse models (7) and (8)**

In the final step, only with changing of the WCONPROD keyword in the simulation software Eclipse the results that can meet expected outcomes are obtained. Figure 3.57 to Figure 3.60 illustrate those produced results.

At the end of this section, the final elapsed CPU and the time to run the simulated fine and coarse models (7) and (8) are reported. As it can be seen, these values for the fine model are more than the other models. Comparing of OIP and pore volume between the three discussed models of the trial (4) are illustrated through Figure 3.61.and Table 3.3. This comparison shows that a small deviation between three cases is acceptable.

4.2.2 85 layers

In this part, the properties of the fine scale model were scaled up with the threshold number of 0.8 and the obtained simulation consequences of the both fine and the coarse models are compared with the results of two simulators, Chevron and TotalFinaElf. Due to the large volume of the 85 layers model, the FrontSim simulator was used to run the simulated models. As mentioned before, because of the feature of this simulator, elapsed time for running the both cases of this study is almost similar. Despite the small differences, the results show that the overall level of agreement is acceptable. The observed differences in the diagrams refer to this fact that different methods use different simulators, procedures, grid sizes, time steps, and strategies. Definition of simulation strategy is one of the most important steps to simulate and running a model. To assign the simulation strategies for this model, I did not define a constant value for oil rate production. It can be a reason for the observed deviation in Figure 3.63 and Figure 3.65 .The presence of injector as well as defining the different rules to choose the control mode may have an impact on the production rate and pressure as well. Through Figure 3.62 to Figure 3.65, the simulation results are compared with each other. Figure 3.66 shows that there is a satisfactory agreement between OIP for the fine and the discussed coarse model.

5 Conclusion

The objective of this study is to verify wavelet upscaling method in property upscaling of two-dimensional (2D) and three-dimensional (3D) fine scale geocellular models, which were obtained from Tenth SPE Comparative Solution Project. This thesis accomplishes several goals.

It demonstrates that the use of wavelet transformation is particularly useful for numerical flow simulation at which the reduction of the property data often becomes necessary. It also demonstrates that this method is applicable for upscaling of rock properties in a multi-scale heterogeneous porous media.

Good accuracy, ease of implementation and efficiency are significantly important aspects of each upscaling method. This method presents a high efficiency, high accuracy and easy for implementation. These are important aspects if a very large fine-grid model is utilized to represent an original geological model. Its efficiency in terms of computation time and memory storage elapsed to run a coarse model compared to the original model is another feature of WT as well. Keeping majority of the geological features after upscaling is another advantage of the method.

The lack of considerable differences between simulation results for the 2D and 3D models of the 1 layer, 20 and 85 layers show the accuracy of the method. In the other hand, this method is applicable to wide ranges of scales from a very small to a very large-scale model in heterogeneous porous media. Moreover, the comparison of the obtained simulation results with two commercial simulators, Chevron, and TotalFinaElf, mentioned in SPE 10 paper represent that the overall level of agreement is good and there is no significant differences between the results. Just small differences exist, which refer to different numerical accuracy of the simulators and different strategies, which have been applied.

6 Reference

- Audigane, P., and Blunt, M. J., “Dual Mesh Method in Upscaling,” SPE 79681 (2003)
- Audigane, P., Blunt, M.J., "Dual mesh method for upscaling in waterflood simulation,” Transport in Porous Media (2004)
- Azizmohammadi, S., and Matthäi, K.S., "Multiresolution Wavelet Based Upscaling of Structured Grids," Peer-reviewed IAMG 2011 (2011)
- Azizmohammadi, S., Dabir, B., and Sahimi, M., “Multiresolution Upscaling of Multiscale Heterogeneous Oil Reservoirs Using Wavelet Transformation,” Amirkabir jurnal,17, 65-D (Chemical Engineering), 71-80, Fall 2006-winter (2007)
- Babaei, M., and King, P. R., "A Comparison Between Wavelet and Renormalization Upscaling Methods and Iterative Upscaling-Downscaling Scheme," SPE 141418 (2011)
- Barker, J.W., and Dupouy, P., "An analysis of dynamic pseudo relative permeability methods,” 5th European Conference on the Mathematics of Oil Recovery, Leoben, Austria (1999)
- Barker, J.W., and Thibeau, S., "A Critical Review of the Use of Pseudo relative Permeabilities for Upscaling,” SPE 35491-PA (1997)
- Chen, Y., and Durlofsky, L.J., “An Ensemble Level upscaling Approach for Efficient Estimation of Fine-Scale Production Using Coarse-Scale Simulation,” SPE 106086 (2007)
- Chen, Y., “Upscaling and subgrid modeling of flow and transport in heterogeneous reservoirs,” Ph.D. thesis (2005)
- Chen, Y., and Durlofsky, L.J., “Adaptive local-global upscaling for general flow scenarios in heterogeneous formations,” Transport in Porous Media (2006a)
- Chen, Y., Durlofsky, L.J., Gerritsen, M., and Wen, X.H., “A coupled local-global Upscaling approach for simulating flow in highly heterogeneous formations,” Advances in Water Resources (2003)
- Christie, M.A., and Blunt, M. J., "Tenth SPE Comparative Solution Project: A Comparison of Upscaling Techniques," SPE 66599 (2001)

- Christie, M.A., et al., "A Renormalization-Based Upscaling Technique for WAG Floods in Heterogeneous Reservoirs," SPE 29127 (1995)
- Christie, M.A.,"Upscaling for Reservoir Simulation," SPE- BP Exploration, 1004 -1010 (1996)
- Chu, L., Schatzinger, R.A., and Tham, M.K., "Application of Wavelet Analysis to Upscaling of Rock Properties," SPE 36517 (1996)
- Darman, N.H., Pickup, G.E., and Sorbie, K.S., "A comparison of two-phase dynamic upscaling methods based on fluid potentials," Computational Geosciences (2002)
- Daubechies, I., "Ten lectures on wavelets, vol. 61 of CBMS-NSF Regional Conference Series in Applied Mathematics," Society for Indus and Applied Mathematics (SIAM) (1992)
- Durlofsky, L. J., "Upscaling and Gridding of Fine Scale Geological Models for Flow Simulation," Stanford University (2005)
- Durlofsky, L. J., "Numerical Calculation of Equivalent Grid Block Permeability Tensors for Heterogeneous Porous Media," Water Resources Research 27, No. 5, 699-708 (1991)
- Durlofsky, L. J., Milliken, W. J., and Bernath, A., "Scale up in the Near-Well Region," SPE61855 (2000)
- Farmer, C. L., "Upscaling: a review," Int. J. Numer. Meth.Fluids (2002)
- Gautier, Y., Blunt, M. J., and Christie, M. A., "Nested Gridding and Streamline-based Simulation for Fast reservoir Performance Prediction," Computational Geosciences, 295-320 (1999)
- Gerritsen, M., and Lambers, J. V., "Integration of local–global upscaling and grid adaptively for simulation of subsurface flow in heterogeneous formations," Computational Geosciences (2008)
- Gerritsen, M.G., and Durlofsky, L.J., "Modeling fluid flow in oil reservoirs," Annual Review of Fluid Mechanics (2005)
- Graps, A., "An Introduction to Wavelets," IEEE Computer Society (1995)
- Guan, L., Du, Y., and Li, L., "Wavelets in Petroleum Industry: Past, Present, and Future," SPE 89952 (2004)

- Guedes, S. S., and Schiozer, D. J., “An Implicit Treatment of Upscaling in Numerical Reservoir Simulation,” SPE 51937 (1999)
- Guérillot, D.R., and Verdière, S., "Different Pressure Grids for Reservoir Simulation in Heterogeneous Reservoirs," SPE 29148 (1995)
- Holden, L., and Lia, O., “A tensor estimator for the homogenization of absolute permeability,” Transport in Porous Media (1992)
- Holden, L., and Nielsen, B.F., “Global upscaling of permeability in heterogeneous reservoirs: the output least squares (OLS) method,” Transport in Porous Media (2000)
- Jansen, F.E., and Kelkar, M.G., "Upscaling of Reservoir Properties Using Wavelets," SPE 39495 (1998)
- King, M.J. et al., “Effective Properties for Flow Calculations,” Transport in Porous Media, 20, Nos. 1 and 2, 169, (1995)
- King, M.J., and Mansfield, M., "Flow Simulation of Geologic Models," SPE Reservoir Evaluation & Engineering (1999)
- King, P. R., "Effective values in averaging," in S. S., Edwards, and P. R. King (eds.), Mathematics in Oil Production (1988)
- King, P. R., “The Use of Renormalization for Calculating Effective Permeability.” Transport in Porous Media, No. 1, 37, (1989)
- King, P. R., Muggeridge, A.H., and Price W.G., "RENORMALIZATION CALCULATIONS OF IMMISCIBLE FLOW." Transport in Porous Media (1993)
- King, P.R., "Oil Companies Make Money with Statistical Physics," Physics World (1996)
- Lamber, J.V., Gerritsen, M. G., and Mallison, B. T., "ACCURATE LOCAL PSCALING WITH VARIABLE COMPACT MULTI-POINT TRANSMISSIBILITY CALCULATIONS,” Computational Geosciences (2008)
- Lee, Jaedong, Ekrem, K., and Kelkar, M.G., "Analytical Upscaling of Permeability for Three-Dimensional Grid Block," SPE 27875 (1996)
- Lu, P., and N. Horne, R., "A Multiresolution Approach to Reservoir Parameter Estimation Using Wavelet Analysis," SPE 62985 (2000)

- Mallat, S., “A Theory for Multiresolution Signal Decomposition: The Wavelet Representation,” IEEE Trans. On Pattern Anal. and Machine Intel., 11, 674-693, (1989)
- Mallat, S., “A Wavelet Tour of Signal Processing,” Academic Press, American Elsevier (2009)
- Mallison, B.T., Chen, Y., Durlofsky, L.J., “Nonlinear two-point flux approximations for simulating subsurface flows with full-tensor anisotropy.” Proceedings of the 10th, EAGE (2006)
- Moridis, G.J., Nikolaou, M., and You, Y., "The Use of Wavelet Transforms in the Solution of Two-Phase Flow Problems," SPE 29144 (1996)
- Nordbotten, J. M., Nogués, J. P., and Celia, M. A., "Appropriate Choice of Average Pressure for Upscaling Relative Permeability in Dynamic Flow Conditions," SPE 113558 (2010)
- Panda, M.N., Mosher, C.C., and Chopra, A.K., "Application of Wavelet Transforms to Reservoir-Data Analysis and Scaling,” SPE 60845 (2000)
- Panda, M.N., Mosher, C.C., and Chopra, A.K., "Application of Wavelet Transforms to Reservoir Data Analysis and Scaling," SPE 36516 (2000)
- Pickup, G. E., and Sorbie, K. S., “The Scaleup of Two-Phase Flow in Porous Media Using Phase Permeability Tensors,” SPE 28586 (1996)
- Pickup, G.E., et al., “Permeability tensors for sedimentary structures.”Mathematical Geology (1994b)
- Rame', M., and Killough, J. E., “A New Approach to the Simulation of Flows in Highly Heterogeneous Porous Media,” SPE (21247) Presented at the SPE Symposium on Reservoir Simulation, Anaheim California, 11-17 February (1991)
- Renard, Ph., and de Marsily, G., “Calculating Equivalent Permeability: A Review,” Advances in Water Resources, 20, Nos. 5-6, 253-278 (1997)
- Sahimi, M., Rasaei, M.R., Ebrahimi, F., and Haghighi, M., "Upscaling of Unstable Miscible Displacements and Multiphase Flows Using Multiresolution Wavelet Transformation,"SPE 93320 (2005)

- Sahni, I., and Horne, R. N., "Multiresolution Wavelet Analysis for Improved Reservoir Description," SPE 87820 (2005)
- Shehata, A. M., El-Banbi, A.H., and Sayyouh, M. H., "Proper Selection of Upscaling Techniques for Different Production Processes," SPE150863 (2012)
- Tanyel, E., “FORMATION EVALUATION USING WAVELET ANALYSIS ON LOGS OF THE CHINJI AND NAGRI FORMATIONS, NORTHERN PAKISTA,” Master Thesis (2006)
- Vetterli, M., and Herley, C., "Wavelets and filter banks: Theory and design," IEEE Trans. Signal Proc. (1992)
- Warren, J. E., and Price, H. S., “Flow in Homogeneous Porous Media,” SPEJ, 153-169 (1961)
- Wen, X.H., Durlofsky, L. J., and Edwards M. G., "Upscaling of channel systems in two dimensions using flow-based grids," Transport in Porous Media (2003)
- Wen, X.H., Durlofsky, L. J., and Edwards, M. G., “Use of Border Regions for Improved Permeability Upscaling,” G. Mathematical Geology (2003b)
- Wen, X.H. and Gomez-Hernandez, J. J., “The Constant Displacement Scheme for Tracking Particles in Heterogeneous Aquifers,” Ground Water, p.135–142 (1996)
- Wen, X.H., Chen, Y., and Durlofsky, L.J., “Efficient 3D implementation of local-global upscaling for reservoir simulation.” to appear in SPE Journal (2006)
- White, C.D., and Horne, R.N., "Computing Absolute Transmissibility in the Presence of Fine-Scale Heterogeneity." SPE 16011 (1987)
- Zhang, P., Pickup, G.E., and Christie, M., "A New Practical Method for Upscaling in Highly Heterogeneous Reservoir Models," SPE 103760 (2008)